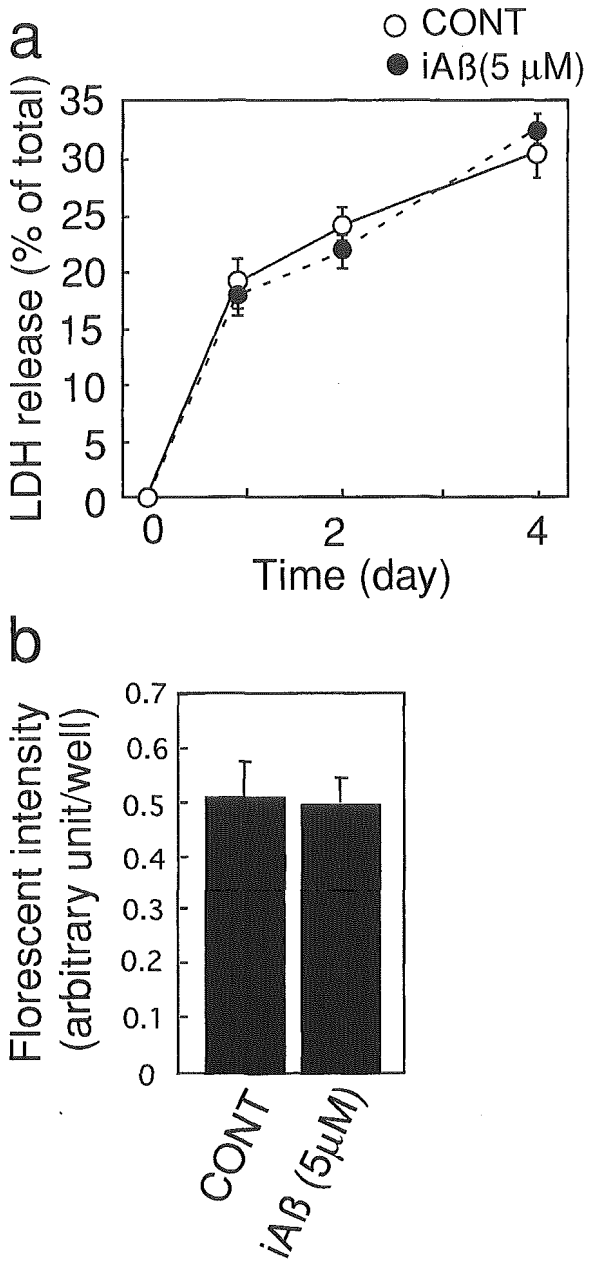

Fig. 5. Effect of iAβ on neuronal viability. **a:** Time course of lactate dehydrogenase (LDH) release into the culture media following incubation with iAβ. The culture media were harvested and subjected to LDH assay at each time point. The data are means ± S.E. for six cultures. **b:** Calcein AM staining was performed on the cultured neurons incubated for 4 days in the presence or absence of iAβ (5 μM). Flourescence intensities of each culture were determined as described in Materials and Methods. The data are means ± S.E. for six cultures.

promotes lipid efflux, inhibits cholesterol synthesis, and reduces cellular cholesterol content, which, in turn, could promote tau phosphorylation and neurodegeneration, as observed in AD brain. Our observations provide new insight into the central issue concerning the pathogenesis of AD, that

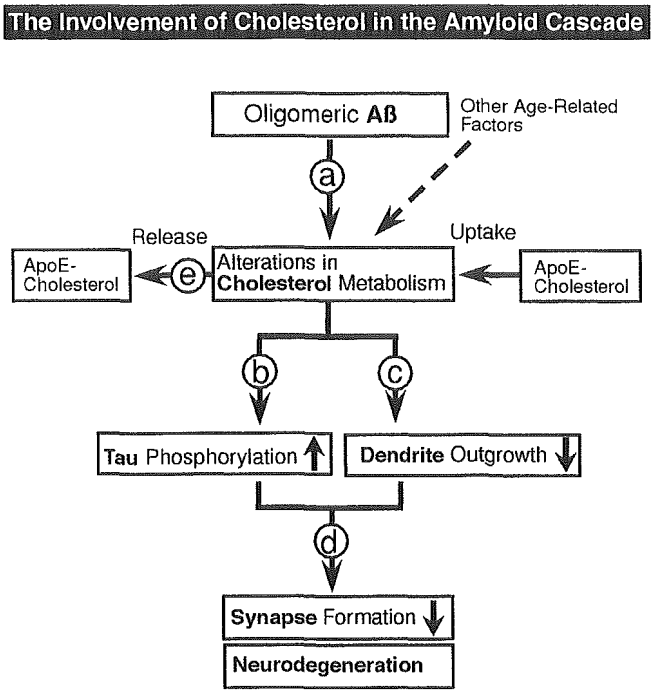

Fig. 6. The putative role of cholesterol in the amyloid cascade. **a:** Oligomeric Aβ reduces cellular cholesterol content in neurons by promoting cholesterol release from neurons to generate Aβ-lipid particles, which are not taken up by neurons (Michikawa et al., 2001) and by inhibiting cholesterol biosynthesis. **b:** The alterations in cholesterol metabolism promote tau phosphorylation in vitro (Fan et al., 2001) and in vivo (Koudinov and Koudinova, 2001; Sawamura et al., 2001). **c, d:** Cholesterol plays an essential role in dendrite outgrowth, synaptic plasticity (Koudinov and Koudinova, 2001; Mauch et al., 2001; Fan et al., 2002), and maintenance of neuronal viability (Michikawa and Yanagisawa, 1999). These lines of evidence support the notion that cholesterol is involved in the mechanism underlying the pathophysiology of Alzheimer's disease (AD) called the amyloid cascade. **e:** ApoE is involved in this cascade by its isoform-dependent difference in the ability to modulate cholesterol metabolism in neurons (Michikawa et al., 2000).

is, the relationship between amyloid plaque formation and the development of neurofibrillary tangles in neurons.

REFERENCES

Andrews NC, Faller DV. 1991. A rapid micropreparation technique for extraction of DNA-binding proteins from limiting numbers of mammalian cells. Nucleic Acids Res 19:2499.

Avdulov NA, Chochina SV, Igbavboa U, Warden CS, Vassiliev AV, Wood WG. 1997. Lipid binding to amyloid β-peptide aggregates: preferential binding of cholesterol as compared with phosphatidylcholine and fatty acids. J Neurochem 69:1746–1752.

Biere AL, Ostaszewski B, Stimson ER, Hyman BT, Maggio JE, Selkoe DJ. 1996. Amyloid β-peptide is transported on lipoproteins and albumin in human plasma. J Biol Chem 271:32916–32922.

Brown MS, Goldstein JL. 1997. The SREBP pathway: regulation of cholesterol metabolism by proteolysis of a membrane-bound transcription factor. Cell 89:331–340.

Busciglio J, Lorenzo A, Yeh J, Yankner BA. 1995. beta-amyloid fibrils induce tau phosphorylation and loss of microtubule binding. Neuron 14:879–888.

Chochina SV, Avdulov NA, Igbavboa U, Cleary JP, O'Hare EO, Wood WG. 2001. Amyloid β-peptide1-40 inreases neuronal membrane fluidity: role of cholesterol and brain region. J Lipid Res 42:1292–1297.

Choo-Smith LP, Garzon-Rodriguez W, Glabe CG, Surewicz WK. 1997. Acceleration of amyloid fibril formation by specific binding of Aβ(1-40) peptide to ganglioside-containing membrane vesicles. J Biol Chem 272: 22987–22990.

El-Agnaf OM, Nagala S, Patel BP, Austen BM. 2001. Non-fibrillar oligomeric species of the amyloid ABri peptide, implicated in familial British dementia, are more potent at inducing apoptotic cell death than protofibrils or mature fibrils. J Mol Biol 310:157–168.

Esiri M, Hyman B, Beyreuther K, Masters C. 1997. Aging and dementia. In: Graham D, Lantos P, editors. Greenfield's neuropathology. London: Arnold. p 153–233.

Fagan AM, Younkin LH, Morris JC, Fryer JD, Cole TG, Younkin SG, Holtzman DM. 2000. Differences in the Aβ40/Aβ42 ratio associated with cerebrospinal fluid lipoproteins as a function of apolipoprotein E genotype. Ann Neurol 48:201–210.

Fan QW, Wei Y, Senda T, Yanagisawa K, Michikawa M. 2001. Cholesterol-dependent modulation of tau phosphorylation in cultured neurons. J Neurochem 76:391–400.

Fan QW, Yu W, Gong JS, Zou K, Sawamura N, Senda T, Yanagisawa K, Michikawa M. 2002. Cholesterol-dependent modulation of dendrite outgrowth and microtubule stability in cultured neurons. J Neurochem 80:178–190.

Fassbender K, Simons M, Bergmann C, Stroick M, Lutjohann D, Keller P, Runz HR, Kuhl S, Bertsch T, von Bergmann K, Hennerici M, Beyreuther K, Hartmann T. 2001. Simvastatin strongly reduces levels of Alzheimer's disease beta-amyloid peptides Abeta 42 and Abeta 40 in vitro and in vivo. Proc Natl Acad Sci USA 98:5856–5861.

Hardy JA, Higgins GA. 1992. Alzheimer's disease: the amyloid cascade hypothesis. Science 256:184–185.

Hartley DM, Walsh DM, Ye CP, Diehl T, Vasquez S, Vassilev PM, Teplow DB, Selkoe DJ. 1999. Protofibrillar intermediates of amyloid β-protein induce acute electrophysiological changes and progressive neurotoxicity in cortical neurons. J Neurosci 19:8876–8884.

Hartmann T. 2001. Cholesterol, Aβ and Alzheimer's disease. Trends Neuorsci 24:S45–48.

Jick HR, Zornberg GL, Jick SS, Seshadri S, Drachman DA. 2000. Statins and the risk of dementia. Lancet 356:1627–1631.

Kojro E, Gimpl G, Lammich S, Marz W, Fahrenholz F. 2001. Low cholesterol stimulates the nonamyloidogenic pathway by its effect on the alpha -secretase ADAM 10. Proc Natl Acad Sci USA 98:5815–5820.

Koudinov A, Matsubara E, Frangione B, Ghiso J. 1994. The soluble form of Alzheimer's amyloid β-protein is complexed to high density lipoprotein 3 and very high density lipoprotein in normal human plasma. Biochem Biophys Res Commun 205:1164–1171.

Koudinov AR, Koudinova NV. 2001. Essential role for cholesterol in synaptic plasticity and neuronal degeneration. FASEB J 15:1858–1860.

Koudinov AR, Koudinova NV, Kumar A, Beavis RC, Ghiso J. 1996. Biochemical characterization of Alzheimer's soluble amyloid β-protein in human cerebrospinal fluid: association with high density lipoproteins. Biochem Biophys Res Commun 223:592–597.

Koudinova NV, Berezov TT, Koudinov AR. 1996. Multiple inhibitory effects of Alzheimer's peptide Aβ1-40 on lipid biosynthesis in cultured human HepG2 cells. FEBS Lett 395:204–206.

Koudinova NV, Koudinov AR, Yavin E. 2000. Alzheimer's Aβ1-40 peptide modulates lipid synthesis in neuronal cultures and intact rat fetal brain under normoxic and oxidative stress conditions. Neurochem Res 25:653–660.

Lambert MP, Barlow AK, Chromy BA, Edwards C, Freed R, Liosatos M, Morgan TE, Rozovsky I, Trommer B, Viola KL, Wals P, Zhang C, Finch CE, Krafft GA, Klein WL. 1998. Diffusible, nonfibrillar ligands derived from Abeta1-42 are potent central nervous system neurotoxins. Proc Natl Acad Sci USA 95:6448–6453.

Launer LJ, White LR, Petrovitch HR, Ross GW, Curb JD. 2001. Cholesterol and neuropathologic markers of AD: a population-based autopsy study. Neurology 57:1447–1452.

Lorenzo A, Yankner BA. 1994. β-amyloid neurotoxicity requires fibril formation and is inhibited by Congo red. Proc Natl Acad Sci USA 91:12243–12247.

Mason RP, Estermyer JD, Kelly JF, Mason PE. 1996. Alzheimer's disease amyloid β-peptide 25-35 is localized in the membrane hydrocarbon core: x-ray diffraction analysis. Biochem Biophys Res Commun 222:78–82.

Mason RP, Jacob RF, Walter MF, Mason PE, Avdulov NA, Chochina SV, Igbavboa U, Wood WG. 1999. Distribution and fluidizing action of soluble and aggregated amyloid β-peptide in rat synaptic plasma membranes. J Biol Chem 274:18801–18807.

Matsubara E, Ghiso J, Frangione B, Amari M, Tomidokoro Y, Ikeda Y, Harigaya Y, Okamoto K, Shoji M. 1999. Lipoprotein-free amyloidogenic peptides in plasma are elevated in patients with sporadic Alzheimer's disease and Down's syndrome. Ann Neurol 45:537–541.

Mattson MP, Tomaselli KJ, Rydel RE. 1993. Calcium-destabilizing and neurodegenerative effects of aggregated β-amyloid peptide are attenuated by basic FGF. Brain Res 621:35–49.

Mauch DH, Nagler K, Schumacher S, Goritz C, Muller EC, Otto A, Pfrieger FW. 2001. CNS synaptogenesis promoted by glia-derived cholesterol. Science 294:1354–1357.

McLaurin J, Chakrabartty A. 1996. Membrane disruption by Alzheimer β-amyloid peptides mediated through specific binding to either phospholipids or gangliosides. Implications for neurotoxicity. J Biol Chem 271: 26482–26489.

Michikawa M, Yanagisawa K. 1998. Apolipoprotein E4 induces neuronal cell death under conditions of suppressed de novo cholesterol synthesis. J Neurosci Res 54:58–67.

Michikawa M, Yanagisawa K. 1999. Inhibition of cholesterol production but not of nonsterol isoprenoid products induces neuronal cell death. J Neurochem 72:2278–2285.

Michikawa M, Fan QW, Isobe I, Yanagisawa K. 2000. Apolipoprotein E exhibits isoform-specific promotion of lipid efflux from astrocytes and neurons in culture. J Neurochem 74:1008–1016.

Michikawa M, Gong JS, Fan QW, Sawamura N, Yanagisawa K. 2001. A novel action of amyloid β-protein (Aβ): oligomeric Aβ promotes lipid efflux. J Neurosci 21:7226–7235.

Muller WE, Koch S, Eckert A, Hartmann HR, Scheuer K. 1995. β-Amyloid peptide decreases membrane fluidity. Brain Res 674:133–136.

Notkola IL, Sulkava R, Pekkanen J, Erkinjuntti T, Ehnholm C, Kivinen P, Tuomilehto J, Nissinen A. 1998. Serum total cholesterol, apolipoprotein E epsilon 4 allele, and Alzheimer's disease. Neuroepidemiology 17:14–20.

Pike CJ, Burdick D, Walencewicz AJ, Glabe CG, Cotman CW. 1993. Neurodegeneration induced by β-amyloid peptides in vitro: the role of peptide assembly state. J Neurosci 13:1676–1687.

Sawamura N, Gong JS, Garver WS, Heidenreich RA, Ninomiya HR, Ohno K, Yanagisawa K, Michikawa M. 2001. Site-specific phosphorylation of tau accompanied by activation of mitogen-activated protein kinase (MAPK) in brains of Niemann-Pick type C mice. J Biol Chem 276:10314–10319.

Selkoe DJ. 1994. Alzheimer's disease: a central role for amyloid. J Neuropathol Exp Neurol 53:438–447.

Simons M, Keller P, De Strooper B, Beyreuther K, Dotti CG, Simons K. 1998. Cholesterol depletion inhibits the generation of β-amyloid in hippocampal neurons. Proc Natl Acad Sci USA 95:6460–6464.

Simons M, Keller P, Dichgans J, Schulz JB. 2001. Cholesterol and Alzheimer's disease: is there a link? Neurology 57:1089–1093.

Takashima A, Noguchi K, Sato K, Hoshino T, Imahori K. 1993. Tau protein kinase I is essential for amyloid beta-protein-induced neurotoxicity. Proc Natl Acad Sci USA 90:7789–7793.

Terzi E, Holzemann G, Seelig J. 1995. Self-association of β-amyloid peptide (1-40) in solution and binding to lipid membranes. J Mol Biol 252:633–642.

Wolozin B, Kellman W, Ruosseau P, Celesia GG, Siegel G. 2000. Decreased prevalence of Alzheimer disease associated with 3-hydroxy-3- methyglutaryl coenzyme A reductase inhibitors. Arch Neurol 57:1439–1443.

Yanagisawa K, Odaka A, Suzuki N, Ihara Y. 1995. GM1 ganglioside-bound amyloid β-protein (Aβ): a possible form of preamyloid in Alzheimer's disease. Nat Med 1:1062–1066.

Yang J, Brown MS, Ho YK, Goldstein JL. 1995. Three different rearrangements in a single intron truncate sterol regulatory element binding protein-2 and produce sterol-resistant phenotype in three cell lines. Role of introns in protein evolution. J Biol Chem 270:12152–12161.

Yip CM, Elton EA, Darabie AA, Morrison MR, McLaurin J. 2001. Cholesterol, a modulator of membrane-associated Abeta-fibrillogenesis and neurotoxicity. J Mol Biol 311:723–734.

Journal of Neurochemistry, 2002, **80**, 178–190

Cholesterol-dependent modulation of dendrite outgrowth and microtubule stability in cultured neurons

Qi-Wen Fan,*,† Wei Yu,‡ Jian-Sheng Gong,* Kun Zou,* Naoya Sawamura,*,§ Takao Senda,† Katsuhiko Yanagisawa* and Makoto Michikawa*

**Department of Dementia Research, National Institute for Longevity Sciences, Aichi, Japan*

†Department of Anatomy, Fujita Health University School of Medicine, Kusukake, Toyoake, Aichi, Japan

‡Departments of Neurology and Anatomy, University of California San Francisco, San Francisco, California, USA

§Japan Science and Technology Corporation (JST), Kawaguchi, Saitama, Japan

Abstract

Microtubule-associated protein 2 (MAP2) is a neuron-specific cytoskeletal protein enriched in dendrites and cell bodies. MAP2 regulates microtubule stability in a phosphorylation-dependent manner, which has been implicated in dendrite outgrowth and branching. We have previously reported that cholesterol deficiency causes tau phosphorylation and microtubule depolymerization in axons (Fan *et al.* 2001). To investigate whether cholesterol also modulates microtubule stability in dendrites by modulating MAP2 phosphorylation, we examined the effect of compactin, a 3-hydroxy-3-methylglutaryl coenzyme A (HMG-CoA) reductase inhibitor, and TU-2078 (TU), a squalene epoxidase inhibitor, on these parameters using cultured neurons. We have found that cholesterol deficiency induced by compactin and TU, inhibited dendrite outgrowth, but not of axons, and attenuated axonal branching. Dephosphorylation of MAP2 and microtubule depolymerization accompanied these alterations. The amount of protein phosphatase 2 A (PP2A) and its activity in association with microtubules were decreased, while those unbound to microtubules were increased. The synthesized ceramide levels and the total ceramide content were increased in these cholesterol-deficient neurons. These alterations caused by compactin were prevented by concurrent treatment of cultured neurons with β-migrating very-low-density lipoproteins (β-VLDL) or cholesterol. Taken together, we propose that cholesterol-deficiency causes a selective inhibition of dendrite outgrowth due to the decreased stability of microtubules as a result of inhibition of MAP2 phosphorylation.

Keywords: axon, cholesterol, dendrite, MAP2, microtubule depolymerization, protein phosphatase 2A.

J. Neurochem. (2002) **80**, 178–190.

During neuronal development and maturation, microtubules undergo rearrangements involving rapid transitions between stable and dynamic states, which are regulated by microtubule-associated protein 2 (MAP2) and other MAPs. MAP2 is selectively enriched in neuronal cell bodies, dendrites, and dendritic spines (Bernhardt and Matus 1984). MAP2 has been postulated to be involved in dendrite outgrowth and contribute to the establishment and maintenance of synaptic connections (Bernhardt and Matus 1984; Aoki and Siekevitz 1985; Dinsmore and Solomon 1991; Caceres *et al.* 1992; Sharma *et al.* 1994). MAP2 has multiple phosphorylation sites for a variety of serine-threonine-directed protein kinases and phosphatases (for review see Sanchez *et al.* 2000b). An increase in the levels of phosphorylated MAP2 is correlated with periods of neurite outgrowth in cultured neurons (Diez-Guerra and Avila 1995) and the development of dendritic branching (Diez-Guerra and Avila 1993b; Craig and Banker 1994). Modifications in the phosphorylation state of MAP2 have been also shown during activity-dependent synaptic specialization in the adult brain (Diez-Guerra and Avila 1993a,1993b). The microtubule-binding affinity of MAP2

Received August 13, 2001; revised manuscript received October 9, 2001; accepted October 13, 2001.

Address correspondence and reprint requests to Makoto Michikawa, Department of Dementia Research, National Institute for Longevity Sciences, 36–3, Gengo, Morioka, Obu, Aichi, 474–8522, Japan.
E-mail: michi@nils.go.jp

Abbreviations used: β-VLDL, β-migrating very-low-density lipoproteins; DMSO, dimethyl sulfoxide; ECL, enhanced chemiluminescence; FITC, fluorescein isothiocyanate; GSK-3β, glycogen synthase kinase-3β; MAP2, microtubule-associated protein 2; MAPK, mitogen-activated protein kinase; PP2A, protein phosphatase 2 A; SDS-PAGE, sodium dodecyl sulfate polyacrylamide gel electrophoresis; SREBP, sterol regulatory element-binding proteins; TS, Tris–saline.

has been shown to be subjected to bidirectional control according to the phosphorylation level of MAP2 (Jameson and Caplow 1981; Nishida *et al.* 1981; Murthy and Flavin 1983; Quinlan and Halpain 1996).

Since the possession of the allele ε4 of apolipoprotein E, which is a key molecule regulating cholesterol metabolism in the central nervous system, was found to be a strong risk factor for the development of Alzheimer's disease (AD), the role of cholesterol in the pathophysiology of AD has been highlighted. Recently, we have found that cholesterol deficiency induces tau phosphorylation and resultant microtubule depolymerization in axons of cultured neurons (Fan *et al.* 2001), and that tau is abnormally phosphorylated in brains of model mice with Niemann–Pick disease type C (Sawamura *et al.* 2001), which is a genetic disorder characterized by lipid storage defects, with deficits in exogenous cholesterol trafficking (Pentchev *et al.* 1995). These findings suggest that cholesterol is the key molecule for maintenance of microtubule stability via the modulation of tau phosphorylation state. Interestingly, several number of studies have shown that a significant loss of dendrite length and MAP2 imunoreactivity are found in AD brains (Flood 1991; Hanks and Flood 1991; Ashford *et al.* 1998). These lines of evidence led us to perform the present experiments in order to examine the role of cholesterol in the regulation of MAP2 phosphorylation, one of the major MAPs other than tau, as well as outgrowth and branching of axons and dendrites in cultured neurons. We show here that cholesterol deficiency causes the polarity-dependent inhibition of dendrite outgrowth, but not of axons, and the inhibition of axonal branching. These morphological alterations were accompanied by microtubule depolymerization in soma and dendrites, as well as highly dephosphorylated MAP2, a decreased amount of protein phosphatase 2 A (PP2A) bound to the microtubules and an increased amount of PP2A not bound to microtubules.

Materials and methods

Antibodies and other reagents

A polyclonal rabbit antibody against MAP2 was kindly provided by Dr Y. Ihara of Tokyo University. Monoclonal antibodies against MAP2 were purchased from Sigma (St Louis, MO, USA) and Leinco Tech Inc. (Ballwin, MO, USA). The monoclonal antibody Tau-1, which recognizes non-phosphorylated sites of tau at four nearby serine residues, Ser195, Ser198, ser199, and Ser202 (numbered as in the longest human tau isoform) (Szendrei *et al.* 1993), was obtained from Boehringer Mannheim (Mannheim, Germany). Monoclonal antibodies against protein phosphatase 2 A (PP2A), β-tubulin, and glycogen synthase kinase-3β (GSK-3β) were purchased from Upstate Biotechnology (Lake Placid, NY, USA), Covance (Richmond, CA, USA), and Transduction Laboratories (Lexington, KY, USA), respectively. Monoclonal antibody against β-tubulin was purchased from Covance. Fluorescein (FITC)-conjugated goat anti-mouse IgG and rhodamine-conjugated affinity-purified goat anti-rabbit IgG were purchased from American Qualex (San Clemente, CA, USA) and Chemicon International Inc. (Temecula, CA, USA), respectively. Horseradish peroxidase-labeled goat anti-rabbit IgG and horseradish peroxidase-labeled goat anti-mouse IgG were purchased from America Quelex and Gibco-BRL Life Technology (Tokyo, Japan), respectively. TU-2078 (TU) was kindly provided by Yoshitomi Pharmaceutical Industries and Tosoh Corporation, Japan (Matsuno *et al.* 1997). Compactin and cholesterol were solubilized in absolute ethanol to prepare stock solutions at concentrations of 10 mM and 10 mg/mL, respectively. TU was solubilized in dimethyl sulfoxide (DMSO) to prepare a stock solution at a concentration of 100 mM. These reagents were directly added into the culture media. Ethanol and DMSO in the stock solutions did not cause any effect on the results of our present studies at concentrations in the culture media used for the experiments.

Cell culture

All experiments were performed in compliance with the relevant laws and institutional guidelines. Cerebral cortical neuronal cultures were prepared from embryonic day-17 Sprague–Dawley rats as previously described (Michikawa and Yanagisawa 1998). The cells were plated onto poly D-lysine-coated glass coverslips for immunocytochemical analysis, 6-well plates for immunoblot analysis, and 12-well plates for the determination of cholesterol content, at a cell density of $1 \times 10^5/cm^2$, $1 \times 10^6/cm^2$, and $1 \times 10^6/cm^2$, respectively. The feeding medium consisted of Dulbecco's modified Eagle's medium nutrient mixture (DMEM : F12; 50 : 50) containing N2 supplement (Bottenstein and Sato 1979) and 0.1% bovine serum albumin (BSA). Six hours after the plating, the cultures were incubated with the reagents to be used in this study until the assays were performed.

Determination of cholesterol and sphingomyelin synthesis

Neurons isolated from cerebral cortices of rat embryos were cultured at a density of 1×10^5 cells/cm^2 on poly-D-lysine-coated 12-well plates. To decrease cellular cholesterol content, two kinds of inhibitors for cholesterol biosynthesis were used. One is an HMG-CoA reductase inhibitor, compactin, and the other is a squalene synthase inhibitor, TU, which selectively exhibits cholesterol synthesis without interfering with synthesis of isoprenoid compounds such as farnesylated proteins, ubiquinone and dolichol. The cultures, maintained in serum-free N2 medium for 6 h, were incubated with various concentrations of compactin or TU. After 24 h of incubation, the cultures were processed for determination of cholesterol and sphingomyelin synthesis using [^{14}C]acetate as a precursor as described previously (Michikawa and Yanagisawa 1998, 1999).

Determination of the cholesterol content in cultured neurons

Neurons isolated from cerebral cortices of rat embryos were cultured at a density of 1×10^6 cells/cm^2 on poly D-lysine-coated 12-well plates. The effects of compactin and TU on cholesterol synthesis were determined as described previously (Michikawa and Yanagisawa 1999). The cultures, maintained in serum-free N2 medium for 6 h were incubated with 300 nM compactin or 10 nM TU in the presence or absence of β-VLDL (70 μg cholesterol/mL) and cholesterol (7 μg/mL), respectively. The cultures were maintained

until harvesting. The amount of cholesterol was determined as described previously (Michikawa and Yanagisawa 1999).

Determination of the ceramide content and ceramide synthesis in cultured neurons

Neurons isolated from cerebral cortices of rat embryos were cultured at a density of 1×10^6 cells/cm^2 on poly D-lysine-coated 6-well plates. The cultures that were maintained in serum-free N2 medium for 6 h were incubated with 300 nM compactin in the presence or absence of cholesterol (7 μg/mL). After 48 h of incubation, the cultures were washed with phosphate-buffered saline (PBS) three times, scraped and collected into Eppendorf tubes. After centrifugation at 7000 *g* for 10 min, the cell pellets were re-suspended in 200 μL of distilled water followed by sonication. The cell homogenate (180 μL) was added into 3 mL of chloroform : methanol (1 : 2 v/v), shaken vigorously, centrifuged at 80 *g* for 5 min, and the organic phase was collected. The organic phase was then evaporated under N2 gas, and the residue was redissolved in 900 μL of chloroform : methanol (1 : 2 v/v) and 100 μL of 1 M NaOH, followed by vigorous shaking and incubation at 37°C for 2 h. Chloroform : methanol (1 : 2 v/v) (100 μL), 1 mL of chloroform and 400 μL of distilled water were added into each sample. After vigorous shaking, the mixtures were centrifuged at 7000 *g* for 10 min. The organic phase was then extracted, evaporated, and then dissolved in chloroform : methanol (1 : 2 v/v). Aliquots of samples normalized by the protein content were spotted on a TLC plate. Ceramide in each sample was separated, heated on a hot plate and quantified using densitometry.

For determination of the level of ceramide synthesis, the cultures that were maintained in serum-free N2 medium for 6 h were incubated with 300 nM compactin in the presence or absence of cholesterol (7 μg/mL). After 48 h of incubation, the cultures were labeled with 2 μCi/mL [^{14}C]acetate for 8 h. The ceramide in the cultures was isolated by the same methods as described above and the activity of labeled ceramide in each sample was quantified using a Bio-imaging Analyzer System-2500 Mac (Fuji Photo Film Co., Ltd, Japan).

Immunocytochemistry

For neuronal immunochemical analysis, the cells were plated and grown on glass coverslips with test reagents. Neurons were fixed in 4% paraformaldehyde for 20 min, permeabilized in 0.2% Triton X-100 for 10 min, and blocked with 5% normal goat serum in PBS for 1 h. The cells were then incubated with primary antibodies in PBS containing 2% BSA overnight at 4°C. The antibodies used were Tau-1 monoclonal antibody (1 : 750 dilution) and anti-MAP2 polyclonal antibody (1 : 500 dilution). For tubulin staining, neurons on coverslips were washed twice with PBS at 37°C. The cells were fixed for 20 min at room temperature in PME buffer (80 mM PIPES, 1 mM $MgCl_2$, 1 mM EGTA) containing a mixture of protease inhibitors, Complete™ (Boehringer Mannheim), 0.2% Triton X-100, 4% paraformaldehyde fluoride, followed rapidly by washing with PBS. The cells were then incubated with the antiβ-tubulin monoclonal antibody (1 : 500 dilution) in PBS containing 2% BSA for 1 h at room temperature, washed four times over a period of 30 min with PBS and incubated for 1 h in secondary antibodies [as appropriate: rhodamine-conjugated goat anti-rabbit IgG (1 : 200), and FITC-conjugated goat anti-mouse IgG (1 : 200)]. The cells were then washed again with PBS and mounted with Vectashield mounting media (Vector Laboratories, Inc., Burlingame, CA, USA). Micrographs were obtained under an Olympus florescent microscope (Olympus, Tokyo, Japan) with an attached Olympus camera using the ×40 objective. Fluorescence images were photographed on 35-mm film and prints were obtained. The lengths of the axons and the number of dendrites and axonal branchings were traced with a digitizer (Wacom, Tokyo, Japan) and analyzed with the aid of a data analysis system (Carl Zeiss Co. Ltd, Jena, Germany). Statistical analyses was performed using StatWiew computer software (Macintosh) and multiple pairwise comparisons among the groups of data were performed using ANOVA and Bonferroni *t*-test.

Immunoblot analysis

Protein samples were lysed and sonicated in RIPA buffer [150 mM NaCl, 10 mM Tris–HCl (pH 7.5), 1% Nonidet p-40, 0.1% sodium dodecyl sulfate (SDS), and 0.25% sodium deoxycholate], containing 1 mM EGTA, a mixture of protease inhibitors, Complete™, and phosphatase inhibitors (10 mM NaF and 1 mM orthovanadate), and centrifuged at 10 000 *g* for 5 min. The protein contents in the clear supernatants were normalized using a BCA protein assay kit and were then subjected to 4–20% gradient Tris/tricine SDS-PAGE (Dia-ichi Pure Chemical Co., Ltd, Tokyo, Japan). The separated proteins were transferred to a polyvinylidene difluoride membrane (Millipore, Bedford, MA, USA). The blots were blocked with 100% Block Ace (Dainippon Pharmacetical Co., Ltd, Osaka, Japan) for 1 h, and incubated with primary antibody for 2 h at room temperature. The first antibodies used were the monoclonal antibodies, anti-Tau1 antibody (1 : 750), antiβ-tubulin antibody (1 : 1000), anti-MAP2 antibody (1 : 500) and anti-PP2A antibody (1 : 1000), and a polyclonal anti-MAP2 antibody (1 : 500). The cells were washed four times over a period of 60 min with PBS-T (PBS containing 0.05% Tween-20), and then incubated with secondary antibodies (horseradish peroxidase-conjugated anti-rabbit or anti-mouse antibodies, diluted 1 : 5000) for 1 h. Between the steps, the blots were washed four times with PBS-T over 15 min. The bound antibodies were detected using enhanced chemilumnescence (ECL; Amersham Pharmacia Biotechnology, Buckinghamshire, UK).

Immunoblot detection of proteins associated with microtubule polymers and soluble tubulin

Soluble tubulin and insoluble microtubule polymers were obtained by scraping the neurons cultured on 6-well plates at 37°C in 100 μL (per well) of microtubule-stabilizing buffer, i.e. PME buffer containing 2 mM GTP, 0.1% Triton X-100, 2 mM dithiothreitol, a mixture of protease inhibitors, Complete™, and phosphatase inhibitors (10 mM NaF and 1 mM orthovanadate). The scraped culture material was sonicated and centrifuged at 100 000 *g* for 60 min at 30°C, resulting in the generation of a supernatant fraction containing soluble tubulin and a pellet fraction containing microtubule polymers. The pellet fractions were solubilized in SDS buffer [62.5 mM Tris–HCl buffer (pH 6.8), containing 2% SDS] at 4°C, followed by sonication to release the bound proteins from the microtubules, and then heated at 90°C for 10 min under reductive conditions. The samples were then centrifuged at 10 000 *g* for 5 min and the protein content of the clear supernatants was determined using the BCA protein assay kit. Equal amounts of the

protein were subjected to 4–20% gradient Tris–tricine SDS-PAGE. The protein contents in the soluble fractions were normalized, diluted with an equal volume of 2 × SDS sampling buffer [62.5 mM Tris–HCl buffer (pH 6.8) that contained 2% SDS, 10% glycerol] containing 5% 2-mercaptoethanol, and subjected to 4–20% gradient Tris–tricine SDS-PAGE. The separated proteins were transferred to a polyvinylidene difluoride membrane (Millipore). The blots were blocked with Block Ace for 1 h and then incubated with primary antibody for 2 h at room temperature. The primary antibodies used were the monoclonal antibodies, anti-PP2A antibody (1 : 2000), anti-β-tubulin antibody (1 : 1000), and anti-GSK-3β antibody (1 : 1000).

Immunoprecipitation and immunoblot detection of PP2A bound to total tubulin

Total tubulin was extracted from neurons by scraping the cells in ice-cold PME buffer that contained a mixture of protease inhibitors, Complete™, and phosphatase inhibitors (10 mM NaF and 1 mM orthovanadate). After incubation on ice for 10 min, the cells were sonicated, and the supernatants were collected after centrifugation at 15 000 *g* for 10 min at 4°C. The protein contents of the clear supernatants were quantified and then equal amounts of protein from each sample were processed for immunoprecipitation. To immunoprecipitate the PP2A bound to tubulin, the supernatant was incubated with 1 μL of mouse monoclonal antibody against PP2A and 100 μL of 20% protein G-Sepharose (Pharmacia) slurry under rotation at 4°C overnight. The immunoprecipitates were solubilized in SDS sampling buffer containing 5% 2-mercaptoethanol by heating at 90°C for 10 min The samples were then centrifuged at 10 000 *g* for 5 min and the clear supernatant was subjected to 4–20% gradient Tris/tricine SDS-PAGE.

Lipoproteins β-VLDL ($d < 1.006$ g/mL) was prepared from the plasma of male New Zealand white rabbits as previously reported (Michikawa and Yanagisawa 1998).

Electron microscopy

Rat embryonic neurons cultured on plastic culture dishes, either untreated or treated with 300 nM compactin at 37°C for 65 h, were prepared for electron microscopy. The cultured neurons were washed with PBS at 37°C and fixed with 2.5% glutaraldehyde in 0.1 M phosphate buffer (pH 7.4) for 20 min, and subsequently with 1% osmium tetroxide in the same buffer for 10 min. After dehydration with graded concentrations of ethanol, the cells were embedded in epoxy resin (Epok812; Oken Shoji, Tokyo). Ultrathin sections were cut in parallel with the dish surface using a diamond knife attached to an ultramicrotome, and placed on copper grids. The sections were double-stained with uranyl acetate and lead citrate, and observed under a transmission electron microscope (H-7100; Hitachi, Tokyo).

Results

Effect of cellular cholesterol levels on the neuronal morphology

In order to study the role of cholesterol in neurite outgrowth in primary neuronal cultures, we examined the effects of inhibitors of cholesterol synthesis, namely, compactin, an HMG-CoA reductase inhibitor, and TU-2078 (TU), an inhibitor of squalene epoxidase, which is located downstream of the branch point for the synthesis of isoprenoid compounds such as farnesylated proteins, ubiquinone and dolichol (Matsuno *et al.* 1997). Neurons cultured in serum-free medium for 72 h in the absence (Fig. 1a) or presence of 300 nM compactin (Fig. 1b), 300 nM compactin plus β-VLDL (70 μg cholesterol/mL) (Fig. 1c), or 300 nM compactin plus cholesterol (7 μg/mL) (Fig. 1d) were double-stained with anti-MAP2 and Tau-1 antibodies. The number of dendrites on the neurons, as represented by MAP2 immunopositivity, was decreased in neuronal cultures treated with compactin (Fig. 1b), whereas such a decrease was not observed in those treated with compactin and β-VLDL (Fig. 1c) or compactin and cholesterol (Fig. 1d). The inhibitory effect of compactin on dendrite outgrowth was also seen in neurons cultured at higher density (Fig. 1g–i). The number of connections between cells was less in cultures treated with 300 nM compactin (Fig. 1h), compared with that observed in control cultures (Fig. 1g) or in those treated with compactin plus cholesterol (Fig. 1i).

Since compactin has been shown to inhibit the synthesis of mevalonate, which is not only a precursor of cholesterol but also of isoprenoid groups that are incorporated into more than a dozen classes of end products, we also studied the effects of TU, a more selective inhibitor of cholesterol synthesis that does not interfere with other critical reactions involving farnesyl pyrophosphate. The effects of treatment of neuronal cultures with 10 nM TU alone or 10 nM TU plus β-VLDL (70 μg cholesterol/mL) are shown in Fig. 1(e,f), respectively. The number of dendrites on neurons was decreased in cultures treated with TU alone (Fig. 1e), but not in those treated with TU plus β-VLDL (Fig. 1f).

To confirm whether these morphological changes in the neurons were correlated with the intracellular cholesterol content, we determined the cholesterol levels in sister cultures. The dose–response curve of the inhibitory effect of compactin and TU on cholesterol synthesis was examined to determine the doses of these compounds to be used in experiments (Fig. 2a and c, respectively). Based on this data, we subsequently used compactin at 300 nM and TU at 10 nM throughout this study. As shown in Fig. 2(b and d), the intracellular cholesterol content in the cultures treated with either compactin (300 nM) or TU (10 nM) alone remained significantly lower throughout the experimental period compared with that measured in control cultures, or in cultures treated with compactin (300 nM) plus β-VLDL (70 μg cholesterol/mL), compactin (300 nM) plus cholesterol (7 μg/mL) (Fig. 2a), TU (10 nM) plus β-VLDL (70 μg cholesterol/mL), or those treated with TU (10 nM) plus cholesterol (7 μg/mL; Fig. 2b). The intracellular cholesterol content in cultures concurrently treated with cholesterol and compactin or TU was even higher than that measured in the control cultures.

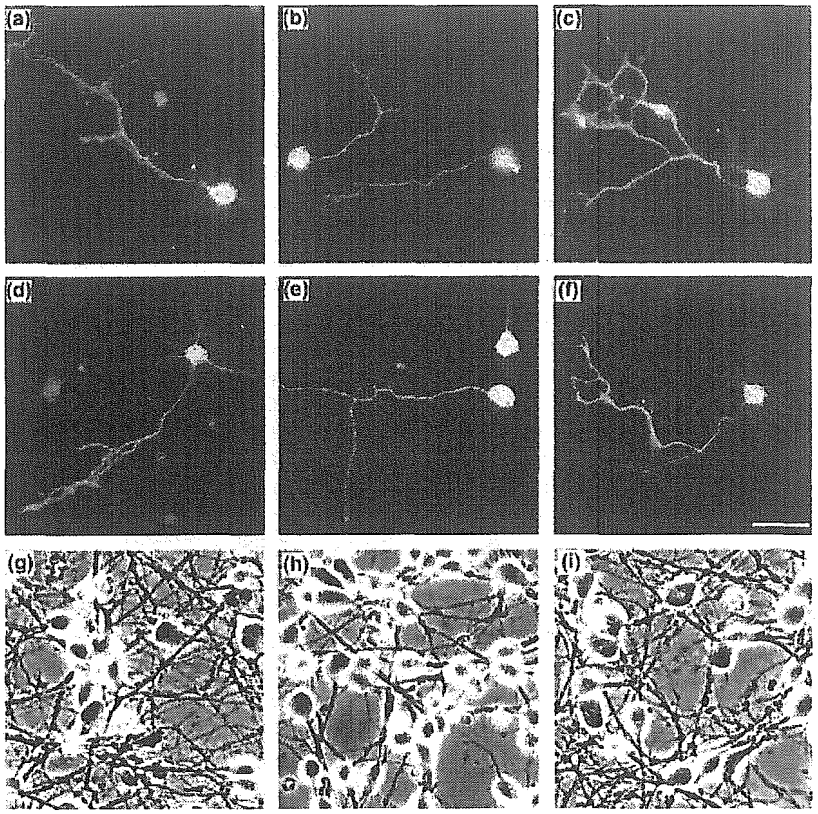

Fig. 1 Effects of compactin and TU on neuronal morphology and their relationship with the intracellular cholesterol content. Neurons maintained for 72 h *in vitro* were double-immunostained with Tau-1 antibody (dephosphorylated-tau, visualized by FITC), and anti-MAP2 antibody (visualized by rhodamine). The number of dendrites on neurons treated with compactin (300 nM) (b) or TU (10 nM) (e) was decreased compared with that in control (a), compactin plus β-VLDL (70 μg cholesterol/mL) (c), compactin plus cholesterol (7 μg/mL) (d), and TU plus β-VLDL (70 μg cholesterol/mL) (f). Photographs of the neuronal cultures plated at a higher density for 72 h are shown in (g–h). The network between cells was poorer in the cultures treated with 300 nM compactin (h), whereas that in the control cultures (g) or with 300 nM compactin plus cholesterol (7 μg/mL) (i) was well developed. Seven independent experiments show similar results. Bar = 20 μm.

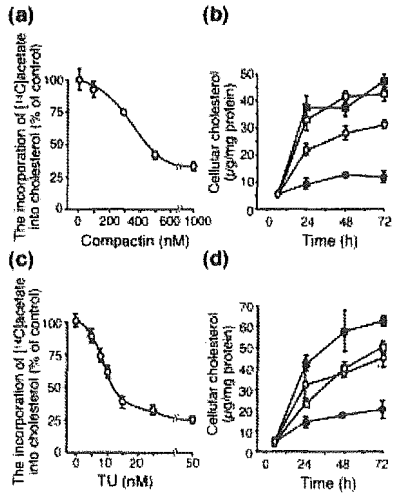

Fig. 2 Effect of compactin and TU on cholesterol synthesis and cellular cholesterol levels in neuronal cultures. Dose–response curves showing inhibitory effect of compactin (a) and TU (c) on cholesterol synthesis. (b) Cellular cholesterol content in the cultures with the reagents; Control (○), 300 nM compactin (●), 300 nM compactin plus β-VLDL (70 μg cholesterol/mL) (□), and 300 nM compactin plus cholesterol (7 μg/mL) (■). (d) Cellular cholesterol content in the cultures with the reagents; Control (○), 10 nM TU (●), 10 nM TU plus β-VLDL (70 μg cholesterol/mL) (□), and 10 nM TU plus cholesterol (7 μg/mL) (■). Data shown are means ± standard error for experiments performed in quadruplicate (a,c) or triplicate (b,d).

Cholesterol-dependent modulation of neurite outgrowth and branching

To investigate in greater detail the organization of neurite outgrowth in neuronal cultures, we analyzed the axonal length, number of axonal branches and number of dendrites in neurons of sister cultures (Fig. 3a–d) compared to treated cultures. The lengths of the axons increased with culture time, with no significant differences observed between control cultures and those treated with compactin alone, or compactin plus β-VLDL (Fig. 3a). However, the number of axonal branches and the number of dendrites on the neurons in the cultures treated with compactin alone were significantly lower than values recorded in control cultures and cultures treated with compactin plus β-VLDL (Fig. 3b and c). Figure 3(d) shows the dose dependence of dendrite outgrowth and axonal elongation following 48 h incubation in the presence of different compactin concentrations; the inhibitory effect of compactin on dendrite outgrowth was dose-dependent, while no effect of compactin on axonal elongation was seen. The axonal length, number of axonal branches and number of dendrites were also determined in control cultures and cultures treated with TU alone or TU plus β-VLDL (Fig. 3e–g). The lengths of the axons increased with culture time, and there were no significant differences among the three types of culture

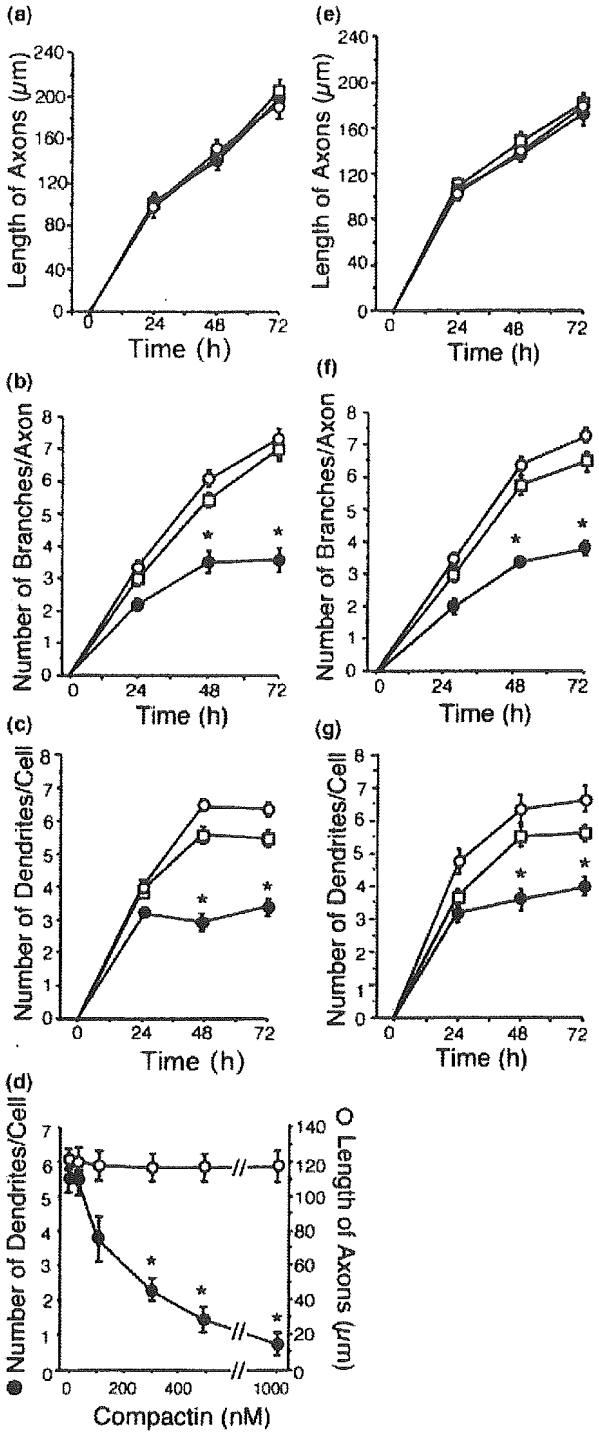

Fig. 3 Effect of compactin and TU on the number of dendrites and axonal branches, and the length of axons. Effect of cholesterol-deficiency induced by compactin on neuronal morphology was analyzed on the neuronal cultures. The treatments were commenced 6 h following plating. Axonal length (a), number of axonal branches (b), and number of dendrites of neurons cultured for 24, 48 and 72 h (c) were analyzed. (d) Dose-dependence of number of dendrites and axonal length on compactin concentrations. Cultures were incubated in Control (○), 300 nM compactin (●), and 300 nM compactin plus β-VLDL (70 μg cholesterol/mL) (□). Effect of cholesterol-deficiency induced by TU on neuronal morphology was analyzed on the neuronal cultures. The treatments were commenced 6 h following plating. Axonal length (e), number of axonal branches (f), and number of dendrites (g) of neurons cultured for 24, 48 and 72 h were analyzed. Cultures were incubated in Control (○), 7.5 nM TU (●), and 7.5 nM TU plus β-VLDL (70 μg cholesterol/mL) (□). The data are the means ± standard error for 40 samples. $^*p < 0.005$ versus control and compactin or TU plus β-VLDL.

conditions (Fig. 3e). However, the number of axonal branches and the number of dendrites in the cultures treated with TU were significantly lower than those in control cultures or cultures treated with TU plus β-VLDL (Fig. 3f and g, respectively).

Effect of cholesterol deficiency on microtubule stability in neurons

Since dendrite outgrowth along with neuronal development and maturation depends on the stability of microtubules, which is regulated by microtubule-associated proteins including MAP2, we next examined the state of microtubules in neuronal cell bodies and dendrites for different culture conditions. Electron micrographs of control neurons and neurons treated with compactin are shown in Fig. 4. It can be seen that continuous microtubule filaments are observed in control neurons (Fig. 4a, arrows), whereas only short fragments of microtubule filaments can be seen in neurons treated with compactin (Fig. 4b, arrows). This indicates that a deficiency in cholesterol reduces microtubule stability in neurons. Furthermore, biochemical examinations were performed to confirm that microtubule stability was affected in cholesterol-deficient neurons. Total, monomeric, and polymerized tubulin were extracted from neuronal cultures incubated with None (control), 300 nM compactin, and 300 nm compactin plus 7 μg/mL cholesterol and then detected by immunoblot analysis. Incubation of cells in N2 medium containing compactin did not significantly affect the quantity of total tubulin as compared with that in cultures grown in N2 medium alone or those treated with compactin plus cholesterol (Fig. 4c). However, a dramatic reduction in the level of polymerized tubulin and a significant increase in the level of monomeric tubulin were observed when the cells were grown in medium containing 300 nM compactin (Fig. 4c). These results indicate that cholesterol deficiency caused by compactin treatment induces microtubule depolymerization.

Effect of cholesterol deficiency on the amount of MAP2 bound or unbound to microtubules

Neuronal cultures were prepared and maintained for 72 h either in the absence of compactin (control), or in the

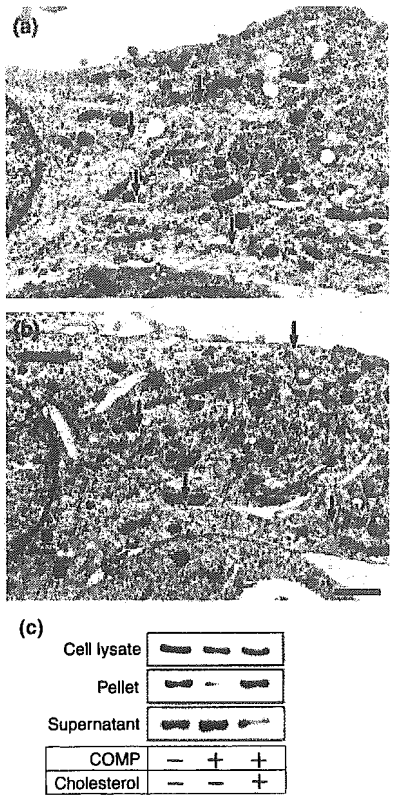

Fig. 4 Electron microscopic study and immunoblot analysis showing microtubule depolymerization in cholesterol-deficient neurons. The neuronal cultures were prepared as described in Materials and Methods. The neurons were treated with compactin at 300 nM and maintained for 72 h. The cultures were washed, fixed and subjected to electron microscopic examination. The microphotographs of negative staining of control neuron (a) and compactin-treated neuron (b) are shown. A number of cell bodies of compactin-treated neurons contained short microtubule fragments (b, arrows) without the normal microtubule formation, while control neurons contain long, continuous microtubules (a, arrows). Bar = 1 μm (c), Immunoblotting of total (cell extract), polymeric (pellet), and monomeric (supernatant) forms of tubulin extracted from neurons. Neuronal cultures were incubated for 65 h in a medium not containing any drug, in medium containing compactin (300 nM), or in a medium containing compactin (300 nM) plus cholesterol (7 μg/mL). Following the incubation, cell extracts were prepared, and monomeric and polymeric forms of tubulin were separated from the cell extract by centrifugation, as described under Materials and Methods. Immunoblot analysis was carried out using antiβ-tubulin antibody. Compactin treatment resulted in significant reduction in the signal in the pellet fraction, while it resulted in an increase in supernatant fraction.

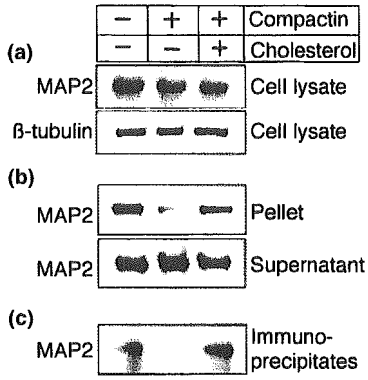

Fig. 5 Total amount of MAP2 and MAP2 in association with microtubules in cholesterol-deficient neurons. The neuronal cultures were prepared and treated 6 h after plating. The cultures were maintained in the presence of 300 nM compactin, 300 nM compactin plus 7 μg/mL of cholesterol or absence of these compounds for 72 h, and harvested with a scraper as described in Materials and Methods. The total cell extract was then subjected to immunoblot analysis with anti-MAP2 or antiβ-tubulin antibody (a). The proteins recovered as pellet or supernatant were analyzed by immunoblotting with anti-AMP2 antibody (b). The total cell extract of each sample was immunoprecipitated with antiβ-tubulin antibody and each immunoprecipitate was subjected to immunoblot analysis with anti-MAP2 antibody (c).

presence of compactin (300 nM), or compactin (300 nM) plus cholesterol (7 μg/mL). The cultures were then harvested and proteins in the microtubule pellet fraction and supernatant fractions were isolated as described in Materials and Methods. As shown in Fig. 5(a), the total amount of MAP2 and β-tubulin remained at similar levels for each of the culture conditions examined. In contrast, the amount of MAP2 bound to microtubules dramatically decreased in the cultures treated with compactin, an effect which was reversed with the addition of cholesterol (Fig. 5b). Neuronal cultures maintained under each of the three conditions were processed for immunoprecipitation with antiβ-tubulin antibody, followed by immunoblot analysis using anti-MAP2 antibody. The amount of MAP2 bound to tubulin was dramatically decreased in the cultures treated with compactin, while in the presence of cholesterol this decrease was not seen (Fig. 5c). At least three independent experiments were performed for each of the culture conditions tested, with consistent results found for each trial.

Suppression of MAP2 phosphorylation in cholesterol-deficient neurons

It is widely believed that MAP2 is one of the major MAPs contributing to microtubules stability, with its ability to promote microtubule assembly modulated by phosphorylation at multiple sites. We therefore examined the phosphorylation state of MAP2 in neurons in the presence or absence of compactin. Phosphorylation efficacy was assayed in control neurons or neurons pre-treated for 48 h with compactin (300 nM), or compactin (300 nM) plus cholesterol (7 μg/mL). The differential regulation of MAP2 phosphorylation in cholesterol-deficient neurons was examined by quantifying ^{32}P incorporation into immunopreci-

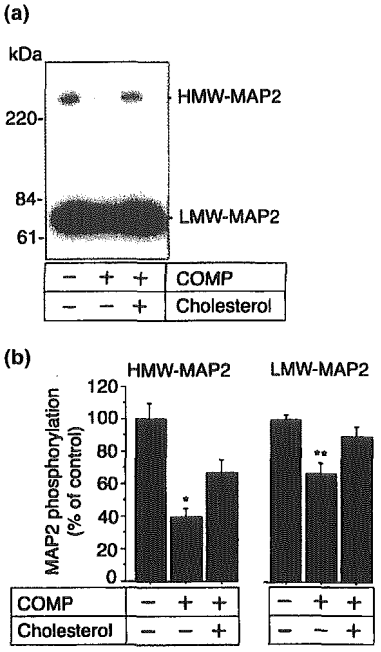

Fig. 6 Suppression of MAP2 phosphorylation in cholesterol-deficient neurons. Neuronal cultures were plated, and either left untreated, or treated with 300 nM compactin (COMP), or 300 nM compactin plus 7 μg/mL cholesterol in serum-free N2 medium, and maintained for 48 h at 37°C. The cells were then washed three times in phosphate-free DMEM and incubated in phosphate-free DMEM for 4 h at 37°C, followed by washing three times with the same medium and incubated with 0.3 mCi/mL of ^{32}P in phosphate-free DMEM for 4 h at 37°C. The cultures were then washed three times in the same medium and cells were harvested with RIPA buffer. Cell extracts were immunoprecipitated with anti-MAP2 antibody over night at 4°C. Each immunoprecipitate was subjected to autoradiography and the intensity of the bands was determined using densitometry. The data indicate the mean ± standard error of samples measured in triplicate. *$p < 0.0005$ versus untreated cultures, *$p < 0.01$ versus COMP + Cholesterol, **$p < 0.002$ versus untreated cultures.

pitated high-molecular-weight (HMW) and low-molecular-weight (LMW) MAP2 in cultures treated as described above. Autoradiography results showed that the amounts of ^{32}P incorporation into both high molecular and low molecular MAP2 were significantly decreased in cultures treated with compactin compared to control cultures and cultures treated with compactin plus cholesterol (Fig. 6a). Three independent experiments were performed and the intensity of each result was quantified densitometrically. The amount of ^{32}P incorporation per μg of MAP2 protein was significantly higher in control cultures compared with cultures treated with compactin or compactin plus cholesterol (Fig. 6b and c, respectively). These data suggest that MAP2 phosphorylation is suppressed in cholesterol-deficient neurons.

Effect of cholesterol-deficiency on the binding of PP2A to microtubules and its activity when in association with microtubules or when unbound

MAP2 phosphorylation is important for the regulation of cytoskeletal function in neurons and is modulated by kinases and phosphatases (Sanchez Martin *et al.* 1998; Sanchez *et al.* 2000a, 2000b). These tau-regulated kinases and phosphatases are known to bind to microtubules and have been suggested to regulate their stability (Sontag *et al.* 1995; Morishima-Kawashima and Kosik 1996; Sanchez *et al.* 2000b). In this way, levels of the putative enzymes glycogen synthase kinase-3β (GSK-3β) and PP2A were examined in light of their capacity to modulate MAP2 phosphorylation. Total tubulin was harvested and immunoprecipitated using antiβ-tubulin antibody in order to determine the total amount of PP2A bound to tubulin. The immunoprecipitates were solubilized and immunoblotted as described in Materials and Methods. As shown in Fig. 7(a), the immunoreactivity of PP2A associated with tubulin was decreased in the cultures treated with compactin or TU. However, this reduction of PP2A immunoreactivity could be reversed by concurrent treatment of cultured cells with cholesterol. In contrast, the immunoreactivity of PP2A in the cell extract did not differ significantly between the different culture conditions. The amount of PP2A bound to tubulin in cultures treated with various concentrations of compactin decreased in a dose-dependent manner (Fig. 7a). In contrast, the amount of PP2A in the cell extract did not differ significantly between the different culture conditions.

Furthermore, we determined the amount of PP2A and GSK-3β bound to microtubules and that not bound to microtubules. Consistent with previous results (Sontag *et al.* 1995, 1996; Merrick *et al.* 1997), we detected PP2A in the microtubule pellet fraction of each culture. As shown in Fig. 7(b), a lower level of PP2A was detected to be bound to microtubules in cultures treated with compactin-only compared to control cultures and those treated with compactin plus β-VLDL or compactin plus cholesterol. The amount of PP2A bound to microtubules in the neurons treated with compactin was significantly reduced compared with that in control cultures, and this effect was reversed by concurrent treatment of cultured cells with β-VLDL or cholesterol (Fig. 7b). In contrast, an increased level of PP2A was detected in the soluble fraction of cultures treated with compactin (Fig. 7b). Using antiβ-tubulin and anti-PP2A antibodies, the levels of tubulin in the pellet fraction and PP2A in the total cell extract were not significantly different for the different culture conditions. In addition, we detected GSK-3β bound to the microtubules. GSK-3β has been shown to be associated with microtubules and phosphorylate MAP2 (Sanchez *et al.* 1996, 2000a). The level of GSK-3β bound to microtubules and in the total cell extract in cultures treated with compactin alone, with compactin plus β-VLDL, or with compactin plus cholesterol were similar to those observed for control cultures (Fig. 7b).

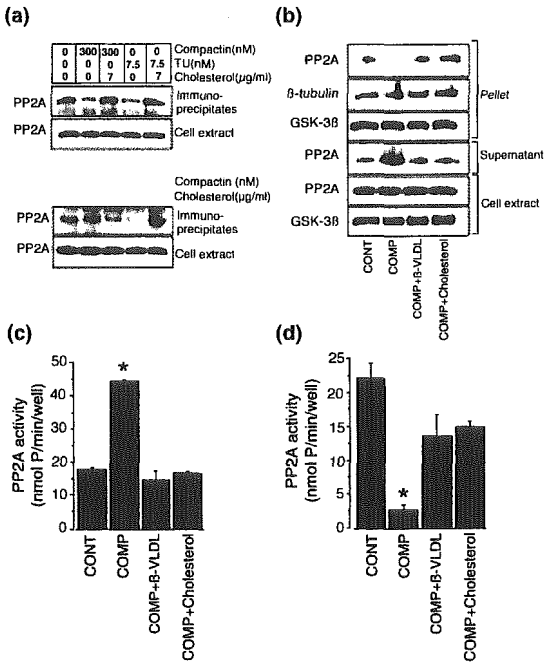

Fig. 7 Binding of PP2A to microtubules and activity of PP2A in association with microtubules or unbound. (a) Neuronal cultures were treated with compactin (300 nM) or TU (7.5 nM) in the absence or presence of cholesterol (7 μg/mL) for 24 h. Another set of neuronal cultures was treated with various concentrations of compactin. Each sample from the extract was immunoprecipitated with antiβ-tubulin antibody over night at 4°C. The immunoprecipitate of each sample was then subjected to immunoblot analysis with anti-PP2A antibody. (b) Neuronal cultures were treated with compactin (300 nM) in the absence or presence of cholesterol (7 μg/mL) or β-VLDL (70 μg/mL cholesterol/mL) for 24 h. The soluble tubulin and insoluble microtubules were obtained by scraping the cultures as described in Materials and Methods. Proteins bound to the microtubules or those in the supernatant were detected by immunoblot analysis. (c) Activity of PP2A in the supernatant was determined using a threonine/serine protein phosphatase assay kit. The activity of PP2A not bound to tubulin was increased in the neuronal cultures treated with compactin (300 nM), an effect that was not observed in cultures treated with compactin plus cholesterol (7 μg/mL) or β-VLDL (70 μg cholesterol/mL). (d) Activity of PP2A bound to microtubules was determined using a threonine/serine protein phosphatase assay kit. The activity of PP2A bound to tubulin was decreased in the neuronal cultures treated with compactin (300 nM), but not in cultures treated with compactin plus cholesterol (7 μg/mL) or β-VLDL (70 μg cholesterol/mL). Phosphatase activity resulting from PP2A was defined as the activity inhibited by 1 nM okadaic acid added into each sample. The data are means ± standard error for experiments performed in triplicate. $^*p < 0.0001$ versus control, COMP + β-VLDL, and COMP + cholesterol.

We next determined PP2A activity in the pellet and supernatant fractions as described in Materials and Methods. A powerful tool in characterizing serine/threonine protein phosphatase activity is the use of okadaic acid as an inhibitor. This compound is a potent inhibitor of protein phosphatase 2 A (IC_{50} = 1 nM), with higher concentrations inhibiting protein phosphatase 1 (IC_{50} = 15–40 nM) (Cohen *et al.* 1989; Haystead *et al.* 1989). Therefore, we used okadaic acid in our assay system as an inhibitor, with phosphatase activity resulting from PP2A defined as the activity inhibited by 1 nM okadaic acid. PP2A activities in aliquots from supernatant fractions of cultures treated with compactin were significantly increased compared to those of control cultures and cultures treated with compactin plus β-VLDL or compactin plus cholesterol (Fig. 7c). In contrast, PP2A activities in aliquots from pellet fractions of cultures treated with compactin were significantly reduced compared to control cultures and cultures treated with compactin plus β-VLDL or compactin plus cholesterol (Fig. 7d).

Effect of cholesterol-deficiency on ceramide synthesis and its content

Since it has been well established that ceramide stimulates PP2A activity (Dobrowsky and Hannun 1992; Dobrowsky *et al.* 1993; Chalfant *et al.* 1999), we examined the effect of compactin on ceramide metabolism to determine whether cholesterol deficiency is responsible for the modulation of PP2A activity. It is known that cholesterol and fatty acids are synthesized by regulated pathways in animal cells, which are influenced by a family of transcription factors called sterol regulatory element-binding proteins (SREBPs) (Brown and Goldstein 1997). Compactin is a competitive inhibitor of HMG-CoA reductase, and the proteolytic processing of SREBPs is enhanced in neuronal cultures incubated with compactin. Since fatty acids are components of ceramide and sphingomyelin, it is reasonable to assume that compactin increases ceramide and sphingomyelin synthesis. As shown in Fig. 8(a), compactin decreased cholesterol synthesis, while it increased sphingomyelin synthesis in a dose-dependent manner, suggesting that ceramide synthesis may also be increased. We next determined the synthesized ceramide levels and total ceramide content in the cultured neurons incubated with compactin at a concentration of 500 nM. As shown in Fig. 8(b and c), compactin increased ceramide synthesis and the total ceramide content in neurons, and the increases were inhibited by the addition of cholesterol.

Discussion

We have shown that cholesterol-deficiency in neurons results in the inhibition of dendrite outgrowth and neurite branching without altering axonal elongation. This selective modulation of morphology in cholesterol-deficient neurons is accompanied by microtubule depolymerization, a decrease in the amount of MAP2 bound to the microtubules, and a decreased level of MAP2 phosphorylation. Moreover, we have shown that PP2A activity in association with microtubules is decreased, while that free from microtubules is increased

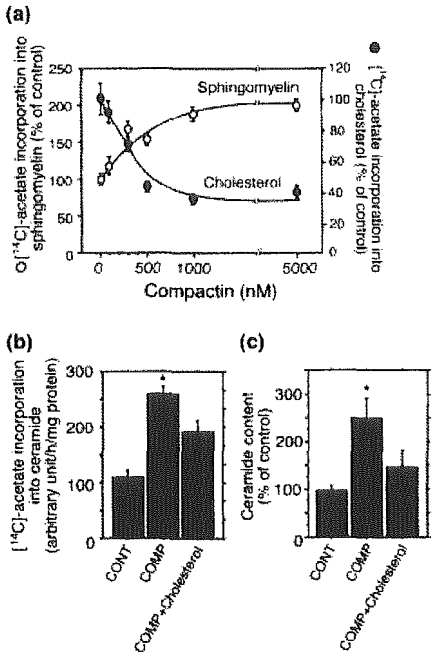

Fig. 8 (a) Neuronal cultures were treated with compactin at various concentrations for 48 h. The cultures were then incubated with 2 μCi/mL [^{14}C]acetate for 8 h and cholesterol synthesis and sphingomyelin synthesis were determined as previously reported (Michikawa and Yanagisawa 1998). (b) For determination of ceramide synthesis, the cultures, maintained in serum-free N2 medium for 6 h, were incubated with 300 nM compactin in the presence or absence of cholesterol (7 μg/mL). After 48 h of incubation, the cultures were labeled with 2 μCi/mL [^{14}C]acetate for 6 h. The ceramide synthesis in the cultures was determined as described under Materials and methods. (c) The cultures maintained in serum-free N2 medium for 6 h were incubated with 300 nM compactin in the presence or absence of cholesterol (7 μg/mL). After 48 h of incubation, the cultures were washed and processed for determination of ceramide content as described under Materials and Methods. The data were mean ± SEM for triplicate (a) or quadruplicate (b and c). *$p < 0.0001$ versus CONT, *$p < 0.02$ versus COMP + Cholesterol (b). *$p < 0.01$ versus COMP (c). Three independent experiments showed similar results.

in these neurons. The increased level of ceramide synthesis accompanied these alterations.

MAP2 is a phosphoprotein whose cellular activities are regulated by phosphorylation and dephosphorylation. The phosphorylation state of MAP2 is modulated by neural activity *in vivo* (Aoki and Siekevitz 1985; Halpain and Greengard 1990; Quinlan and Halpain 1996). Previous reports on studies carried out *in vitro* have shown that, based on the structural changes that occur in MAP2 with increasing phosphorylation and the fact that MAP2 is largely confined to neuronal dendrites, increasing phosphorylation of MAP2 promotes increased branching (Friedrich and Aszodi 1991). It has been demonstrated that the phosphorylation state of MAP2 determines its binding to microtubules: neither dephosphorylated nor hyperphosphorylated MAP2 bind to microtubules, and phosphorylation of certain sites in MAP2 is essential for it being able to bind to microtubules (Brugg and Matus 1991). Therefore, it may be possible that cholesterol deficiency inhibits the phosphorylation of MAP2, which in turn would lead to the inhibition of binding of MAP2 to micotubules, microtubule depolymerization, and inhibition of dendrite outgrowth.

A discrepancy between the effects of cholesterol-deficiency on the outgrowth of dendrites and that of axons was observed in the present study: a decreased cholesterol level inhibited dendrite outgrowth while it seemed to have little effect on axonal outgrowth (Figs 1 and 2). A possible explanation for this discrepancy could be correlated with the difference in the phosphorylation levels between HMW and LMW MAP2. Previous studies have shown that the HMW form of MAP2 is found only in neurons that have commenced dendrogenesis and is more abundant in dendrites than in axons, and that HMW MAP2 plays a fundamental role in the formation of dendrites (Bernhardt and Matus 1982, 1984; Vallee 1982; Caceres *et al.* 1984; Tucker *et al.* 1988). Consistent with these lines of evidence, the selective inhibition of dendrite outgrowth and not of axonal elongation demonstrated in the present study is correlated with the differences in the levels of phosphorylation between HMW and LMW MAP2 observed here; the reduction in the levels of HMW MAP2 phosphorylation was more prominent than that of LMW MAP2.

Another possible explanation for the differential requirement of cholesterol in dendritic compared with axonal development may relate to the difference in microtubule organization in these two neuronal compartments. A previous report has demonstrated that microtubules in axons have all their plus ends pointing distally, while dendrites have microtubules oriented in both orientations (for review see Baas 1999). It may be possible that minus-end distal microtubules are particularly sensitive to perturbations in cholesterol content. Recently, it has been demonstrated that Lis1 protein regulates dynein behavior and microtubule organization, and is thus essential for dendritic morphogenesis but not for axonal morphogenesis (Liu *et al.* 2000; Smith *et al.* 2000). Taking these results into account, cholesterol might be involved in the modulation of activity of some proteins, such as Lis1, which are essential for dendritic morphogenesis.

It has been shown that highly phosphorylated MAP2 is unbound to mictrotubules and is recovered in soluble fractions (Sanchez *et al.* 2000a). In contrast, our present data indicate that dephosphorylated MAP2 cannot bind to microtubules and is recovered in the soluble fraction (Fig. 5). These contradictory phenomena can be explained by the assumption made in a previous study that neither highly phosphorylated MAP2 nor highly dephosphorylated MAP2 could bind to tubulin (Brugg and Matus 1991). The question naturally arises from these results as to how cholesterol

modulates the phosphorylation state of MAP2 in neurons. Our present results indicate that cholesterol deficiency stimulates ceramide synthesis and increases ceramide content (Fig. 8b,c). As previous findings have shown that ceramide enhances PP1 and PP2A activity (Dobrowsky and Hannun 1992; Dobrowsky *et al.* 1993), one possible explanation to this question is that increases in the ceramide synthesis and its content, which are induced by treatment with compactin, activate PP2A in neurons. It is well known that proteolytic processing of SREBPs is regulated by the membrane cholesterol content (Brown and Goldstein 1997). The N-terminal domains of the SREBPs are released from membranes and travel to the nucleus to enhance multiple genes encoding enzymes of cholesterol synthesis, unsaturated fatty acid synthesis, triglyceride synthesis, and lipid uptake (see review Horton and Shimomura 1999). Thus, the enhancement of proteolytic process of SREBPs by compactin treatment not only increases the expression level of HMG-CoA reductase but also the fatty acid synthesis. Since the increased levels of fatty acids are known to promote ceramide and sphingomyelin synthesis, it is reasonable to postulate that cholesterol deficiency caused by compactin increases fatty acid and ceramide synthesis, leading to the activation of PP2A.

The present study has demonstrated that the increase in PP2A not bound to microtubules is the most prominent alteration we have observed. It has been reported that the catalytic subunit of PP2A is inhibited by its binding to microtubules, which could be a competitive inhibitor for PP2A to bind to the same region on tau (Sontag *et al.* 1999), suggesting that PP2A can efficiently dephosphorylate tau only when neither protein is bound to microtubules. The interaction site of tau for PP2A corresponds approximately to amino acid residues 221–396, which encompasses the microtubule-binding repeats (Drewes *et al.* 1998). Since the C-terminal microtubule-binding domain is known to be quite well conserved between the MAPs, including tau and MAP2 (Drewes *et al.* 1998), it may be possible to postulate that PP2A efficiently dephosphorylates MAP2 which is free from microtubules. If this is the case, the increased amount of both PP2A and MAP2 detached from microtubules could explain why MAP2 is highly dephosphorylated in cholesterol-deficient neurons, because the amount of PP2A free from microtubules was increased in cholesterol-deficient cultures. Thus, the decreased level of MAP2 protein, which is phosphorylated to a certain degree at certain sites required for exhibiting a microtubule-binding action that stabilizes cell structure, may induce instability of microtubules and resultant inhibition of dendrite outgrowth.

The last question to be addressed is why an increased amount of PP2A unbound from microtubules did not dephosphorylate tau. Actually, at present, we do not have any direct evidence that can explain this polarity-specific discrepancy that MAP2 is dephosphorylated in somata and dendrites, while tau is hyperphosphorylated (Fan *et al.* 2001), and that despite the defect in dendritic morphogenesis in cholesterol-deficient neurons, elongation of axons was normal, as shown in Fig. 3. Possible explanations for this discrepancy might be that the elevation of free PP2A levels detected in supernatant fraction reflect mainly that of somatodendritic domains but not that of axonal domains, or that the balance between kinase and phosphatase activities may be differently affected by cholesterol deficiency in axonal and somatodendritic domains. Although the precise mechanism remains unknown, the role of cholesterol in the formation of polarity-specific sorting domains called rafts, and the importance of cholesterol in the intracellular traffic, the formation of membrane polarity and the maintenance of cell functions, including signal transduction, have been demonstrated (Hannan and Edidin 1996; Ledesma *et al.* 1998; Simons and Toomre 2000). Thus, it may not be surprising that cholesterol deficiency induces opposite phosphorylation states of tau and MAP2, which stabilize microtubules in axonal and somatodendritic domains, respectively. Although, further studies are required to elucidate the precise mechanism(s) underlying cholesterol-dependent and polarity-specific modulations of phosphorylation of MAPs, our observations in the present study provide new insights into the role of cholesterol in modulation of dendritic and therefore synaptic remodelling and tau phosphorylation which are central processes of relevance to the biology of neurons of AD brains.

Acknowledgements

This study was supported by a research grant for Longevity Sciences (8 A-1), Research on Brain Science from Ministry of Health and Welfare, and by CREST (Core Research for Evolutional Sciences and Technology), Japan, and by Brain Science foundation and Life Science Foundation of Japan.

References

Aoki C. and Siekevitz P. (1985) Ontogenetic changes in the cyclic adenosine 3′,5′-monophosphate- stimulatable phosphorylation of cat visual cortex proteins, particularly of microtubule-associated protein 2 (MAP 2): effects of normal and dark rearing and of the exposure to light. *J. Neurosci.* **5**, 2465–2483.

Ashford J. W., Soultanian N. S., Zhang S. X. and Geddes J. W. (1998) Neuropil threads are collinear with MAP2 immunostaining in neuronal dendrites of Alzheimer brain. *J. Neuropathol. Exp. Neurol.* **57**, 972–978.

Baas P. W. (1999) Microtubules and neuronal polarity: lessons from mitosis. *Neuron* **22**, 23–31.

Bernhardt R. and Matus A. (1982) Initial phase of dendrite growth: evidence for the involvement of high molecular weight microtubule-associated proteins (HMWP) before the appearance of tubulin. *J. Cell Biol.* **92**, 589–593.

Bernhardt R. and Matus A. (1984) Light and electron microscopic studies of the distribution of microtubule-associated protein 2 in rat brain: a difference between dendritic and axonal cytoskeletons. *J. Comp Neurol.* **226**, 203–221.

Bottenstein J. E. and Sato G. H. (1979) Growth of a rat neuroblastoma cell line in serum-free supplemented medium. *Proc. Natl. Acad. Sci. USA* **76**, 514–517.

Brown M. S. and Goldstein J. L. (1997) The SREBP pathway: regulation of cholesterol metabolism by proteolysis of a membrane-bound transcription factor. *Cell* **89**, 331–340.

Brugg B. and Matus A. (1991) Phosphorylation determines the binding of microtubule-associated protein 2 (MAP2) to microtubules in living cells. *J. Cell Biol.* **114**, 735–743.

Caceres A., Binder L. I., Payne M. R., Bender P., Rebhun L. and Steward O. (1984) Differential subcellular localization of tubulin and the microtubule-associated protein MAP2 in brain tissue as revealed by immunocytochemistry with monoclonal hybridoma antibodies. *J. Neurosci.* **4**, 394–410.

Caceres A., Mautino J. and Kosik K. S. (1992) Suppression of MAP2 in cultured cerebellar macroneurons inhibits minor neurite formation. *Neuron* **9**, 607–618.

Chalfant C. E., Kishikawa K., Mumby M. C., Kamibayashi C., Bielawska A. and Hannun Y. A. (1999) Long-chain ceramides activate protein phosphatase-1 and protein phosphatase-2A. Activation is stereospecific and regulated by phosphatidic acid. *J. Biol. Chem.* **274**, 20313–20317.

Cohen P., Klumpp S. and Schelling D. L. (1989) An improved procedure for identifying and quantitating protein phosphatases in mammalian tissues. *FEBS Lett.* **250**, 596–600.

Craig A. M. and Banker G. (1994) Neuronal polarity. *Annu. Rev. Neurosci.* **17**, 267–310.

Diez-Guerra F. J. and Avila J. (1993a) Rapid dephosphorylation of microtubule-associated protein 2 in the rat brain hippocampus after pentylenetetrazole-induced seizures. *Eur. J. Biochem.* **215**, 181–187.

Diez-Guerra F. J. and Avila J. (1993b) MAP2 phosphorylation parallels dendrite arborization in hippocampal neurones in culture. *Neuroreport* **4**, 419–422.

Diez-Guerra F. J. and Avila J. (1995) An increase in phosphorylation of microtubule-associated protein 2 accompanies dendrite extension during the differentiation of cultured hippocampal neurones. *Eur. J. Biochem.* **227**, 68–77.

Dinsmore J. H. and Solomon F. (1991) Inhibition of MAP2 expression affects both morphological and cell division phenotypes of neuronal differentiation. *Cell* **64**, 817–826.

Dobrowsky R. T. and Hannun Y. A. (1992) Ceramide stimulates a cytosolic protein phosphatase. *J. Biol. Chem.* **267**, 5048–5051.

Dobrowsky R. T., Kamibayashi C., Mumby M. C. and Hannun Y. A. (1993) Ceramide activates heterotrimeric protein phosphatase 2A. *J. Biol. Chem.* **268**, 15523–15530.

Drewes G., Ebneth A. and Mandelkow E. M. (1998) MAPs, MARKs and microtubule dynamics. *Trends Biochem. Sci.* **23**, 307–311.

Fan Q. W., Wei Y., Senda T., Yanagisawa K. and Michikawa M. (2001) Cholesterol-dependent modulation of tau phosphorylation in cultured neurons. *J. Neurochem.* **76**, 1–11.

Flood D. G. (1991) Region-specific stability of dendritic extent in normal human aging and regression in Alzheimer's disease. II. Subiculum. *Brain Res.* **540**, 83–95.

Friedrich P. and Aszodi A. (1991) MAP2: a sensitive cross-linker and adjustable spacer in dendritic architecture. *FEBS Lett.* **295**, 5–9.

Halpain S. and Greengard P. (1990) Activation of NMDA receptors induces rapid dephosphorylation of the cytoskeletal protein MAP2. *Neuron* **5**, 237–246.

Hanks S. D. and Flood D. G. (1991) Region-specific stability of dendritic extent in normal human aging and regression in Alzheimer's disease. I. CA1 of hippocampus. *Brain Res.* **540**, 63–82.

Hannan L. A. and Edidin M. (1996) Traffic, polarity, and detergent solubility of a glycosylphosphatidylinositol-anchored protein after LDL-deprivation of MDCK cells. *J. Cell Biol.* **133**, 1265–1276.

Haystead T. A., Sim A. T., Carling D., Honnor R. C., Tsukitani Y., Cohen P. and Hardie D. G. (1989) Effects of the tumour promoter okadaic acid on intracellular protein phosphorylation and metabolism. *Nature* **337**, 78–81.

Horton J. D. and Shimomura I. (1999) Sterol regulatory element-binding proteins: activators of cholesterol and fatty acid biosynthesis. *Curr. Opin. Lipidol.* **10**, 143–150.

Jameson L. and Caplow M. (1981) Modification of microtubule steady-state dynamics by phosphorylation of the microtubule-associated proteins. *Proc. Natl. Acad. Sci. USA* **78**, 3413–3417.

Ledesma M. D., Simons K. and Dotti C. G. (1998) Neuronal polarity: essential role of protein–lipid complexes in axonal sorting. *Proc. Natl. Acad. Sci. USA* **95**, 3966–3971.

Liu Z., Steward R. and Luo L. (2000) Drosophila Lis1 is required for neuroblast proliferation, dendritic elaboration and axonal transport. *Nat. Cell Biol.* **2**, 776–783.

Matsuno T., Kato M., Tsuchida Y., Takahashi M., Yaguchi S. and Terada S. (1997) Synthesis and aromatase-inhibitory activity of imidazolyl-1,3,5- triazine derivatives. *Chem. Pharm. Bull.* **45**, 291–296.

Merrick S. E., Trojanowski J. Q. and Lee V. M. (1997) Selective destruction of stable microtubules and axons by inhibitors of protein serine/threonine phosphatases in cultured human neurons. *J. Neurosci.* **17**, 5726–5737.

Michikawa M. and Yanagisawa K. (1998) Apolipoprotein E4 induces neuronal cell death under conditions of suppressed de novo cholesterol synthesis. *J. Neurosci. Res.* **54**, 58–67.

Michikawa M. and Yanagisawa K. (1999) Inhibition of cholesterol production but not of nonsterol isoprenoid products induces neuronal cell death. *J. Neurochem.* **72**, 2278–2285.

Morishima-Kawashima M. and Kosik K. S. (1996) The pool of MAP kinase associated with microtubules is small but constitutively active. *Mol. Biol. Cell* **7**, 895.

Murthy A. S. and Flavin M. (1983) Microtubule assembly using the microtubule-associated protein MAP-2 prepared in defined states of phosphorylation with protein kinase and phosphatase. *Eur. J. Biochem.* **137**, 37–46.

Nishida E., Kuwaki T. and Sakai H. (1981) Phosphorylation of microtubule-associated proteins (MAPs) and pH of the medium control interaction between MAPs and actin filaments. *J. Biochem.* **90**, 575–578.

Pentchev P. G., Vanier M. T., Suzuki K. and Patterson M. C. (1995) Niemann-Pick disease, type C: a cellualr cholesterol lipidosis. In: The Metabolic and Molecular Basis of Inherited Disease (Scriver, C. R., Beaudet, A. L., Sly, W. S., Valle, D., eds), pp. 2625–2640. New York: McGraw-Hill.

Quinlan E. M. and Halpain S. (1996) Emergence of activity-dependent, bidirectional control of microtubule-associated protein MAP2 phosphorylation during post-natal development. *J. Neurosci.* **16**, 7627–7637.

Sanchez C., Diaz-Nido J. and Avila J. (2000b) Phosphorylation of microtubule-associated protein 2 (MAP2) and its relevance for the regulation of the neuronal cytoskeleton function. *Prog. Neurobiol.* **61**, 133–168.

Sanchez Martin C., Diaz-Nido J. and Avila J. (1998) Regulation of a site-specific phosphorylation of the microtubule-associated protein 2 during the development of cultured neurons. *Neuroscience* **87**, 861–870.

Sanchez C., Perez M. and Avila J. (2000a) GSK3β-mediated phosphorylation of the microtubule-associated protein 2C (MAP2C) prevents microtubule bundling. *Eur. J. Cell Biol.* **79**, 252–260.

Sanchez C., Tompa P., Szucs K., Friedrich P. and Avila J. (1996) Phosphorylation and dephosphorylation in the proline-rich

C-terminal domain of microtubule-associated protein 2. *Eur. J. Biochem.* **241**, 765–771.

Sawamura N., Gong J. S., Garver W. S., Heidenreich R. A., Ninomiya H., Ohno K., Yanagisawa K. and Michikawa M. (2001) Site-specific phosphorylation of tau accompanied by activation of mitogen-activated protein kinase (MAPK) in brains of Niemann–Pick type C mice. *J. Biol. Chem.* **276**, 10314–10319.

Sharma N., Kress Y. and Shafit-Zagardo B. (1994) Antisense MAP-2 oligonucleotides induce changes in microtubule assembly and neuritic elongation in pre-existing neurites of rat cortical neurons. *Cell Motil. Cytoskeleton* **27**, 234–247.

Simons K. and Toomre D. (2000) Lipid rafts and signal transduction. *Nat. Rev. Mol. Cell Biol.* **1**, 31–39.

Smith D. S., Niethammer M., Ayala R., Zhou Y., Gambello M. J., Wynshaw-Boris A. and Tsai L. H. (2000) Regulation of cytoplasmic dynein behaviour and microtubule organization by mammalian Lis1. *Nat. Cell Biol.* **2**, 767–775.

Sontag E., Nunbhakdi-Craig V., Bloom G. S. and Mumby M. C. (1995) A novel pool of protein phosphatase 2A is associated with microtubules and is regulated during the cell cycle. *J. Cell Biol.* **128**, 1131–1144.

Sontag E., Nunbhakdi-Craig V., Lee G., Bloom G. S. and Mumby M. C. (1996) Regulation of the phosphorylation state and microtubule-binding activity of Tau by protein phosphatase 2A. *Neuron* **17**, 1201–1207.

Sontag E., Nunbhakdi-Craig V., Lee G., Brandt R., Kamibayashi C., Kuret J., White C. L., 3rd Mumby M. C. and Bloom G. S. (1999) Molecular interactions among protein phosphatase 2A, tau, and microtubules. Implications for the regulation of tau phosphorylation and the development of tauopathies. *J. Biol. Chem.* **274**, 25490–25498.

Szendrei G. I., Lee V. M. and Otvos L. Jr (1993) Recognition of the minimal epitope of monoclonal antibody Tau-1 depends upon the presence of a phosphate group but not its location. *J. Neurochem.* **34**, 243–249.

Tucker R. P., Binder L. I., Viereck C., Hemmings B. A. and Matus A. I. (1988) The sequential appearance of low- and high-molecular-weight forms of MAP2 in the developing cerebellum. *J. Neurosci.* **8**, 4503–4512.

Vallee R. B. (1982) A taxol-dependent procedure for the isolation of microtubules and microtubule-associated proteins (MAPs). *J. Cell Biol.* **92**, 435–442.

THE JOURNAL OF BIOLOGICAL CHEMISTRY
Vol. 277, No. 33, Issue of August 16, pp. 29919–29926, 2002

Printed in U.S.A.

Apolipoprotein E (ApoE) Isoform-dependent Lipid Release from Astrocytes Prepared from Human ApoE3 and ApoE4 Knock-in Mice*

Received for publication, April 23, 2002, and in revised form, May 31, 2002
Published, JBC Papers in Press, May 31, 2002, DOI 10.1074/jbc.M203934200

Jian-Sheng Gong‡§, Mariko Kobayashi¶, Hideki Hayashi‡, Kun Zou‡, Naoya Sawamura‡‖, Shinobu C. Fujita¶, Katsuhiko Yanagisawa‡, and Makoto Michikawa‡**

From the ‡Department of Dementia Research, National Institute for Longevity Sciences, 36-3 Gengo, Morioka, Obu, Aichi 474-8522, Japan, the §Organization for Pharmaceutical Safety and Research of Japan, Tokyo 100-0013, Japan, ¶Mitsubishi Kagaku Institute of Life Sciences, 11 Minamiooya, Machida, Tokyo 194-8511, Japan, and ‖Japan Society for the Promotion of Science (JSPS), Tokyo 102-8471, Japan

We have reported previously (Michikawa, M., Fan, Q.-W., Isobe, I., and Yanagisawa, K. (2000) *J. Neurochem.* 74, 1008–1016) that exogenously added recombinant human apolipoprotein E (apoE) promotes cholesterol release in an isoform-dependent manner. However, the molecular mechanism underlying this isoform-dependent promotion of cholesterol release remains undetermined. In this study, we demonstrate that the cholesterol release is mediated by endogenously synthesized and secreted apoE isoforms and clarify the mechanism underlying this apoE isoform-dependent cholesterol release using cultured astrocytes prepared from human apoE3 and apoE4 knock-in mice. Cholesterol and phospholipids were released into the culture media, resulting in the generation of two types of high density lipoprotein (HDL)-like particles; one was associated with apoE and the other with apoJ. The amount of cholesterol released into the culture media from the apoE3-expressing astrocytes was ~2.5-fold greater than that from apoE4-expressing astrocytes. In contrast, the amount of apoE3 released in association with the HDL-like particles was similar to that of apoE4, and the sizes of the HDL-like particles released from apoE3- and apoE4-expressing astrocytes were similar. The molar ratios of cholesterol to apoE in the HDL fraction of the culture media of apoE3- and apoE4-expressing astrocytes were 250 ± 6.0 and 119 ± 5.1, respectively. These data indicate that apoE3 has an ability to generate similarly sized lipid particles with less number of apoE molecules than apoE4, suggesting that apoE3-expressing astrocytes can supply more cholesterol to neurons than apoE4-expressing astrocytes. These findings provide a new insight into the issue concerning the putative alteration of apoE-related cholesterol metabolism in Alzheimer's disease.

Previous epidemiological studies show that an elevated serum cholesterol level is a risk factor for the development of Alzheimer's disease (AD)[1] (1–3) and that statin therapy reduces the frequency of AD (4) and dementia (5). The decreased levels of cellular cholesterol have been shown to reduce Aβ production *in vitro* (6) and *in vivo* (7). Previous studies have also shown the association of cholesterol accumulation with mature senile plaques (8) and neurofibrillary tangle-bearing neurons (9). Additionally, a recent study (10) has suggested that an increased cholesterol level in the membrane facilitates amyloid fibril formation through formation of GM1 ganglioside-bound Aβ, a putative endogenous seed. These findings suggest that increased cellular cholesterol levels induce high amyloid β-protein (Aβ) production and subsequent AD development.

However, several studies (11–14) have shown opposing evidence indicating that cholesterol levels in serum, cell membranes of brains, and cerebrospinal fluid are decreased in AD patients compared with those in controls. Previous studies have shown that increased dietary cholesterol levels reduce Aβ secretion (15) and that increased cellular cholesterol levels inhibit the Aβ-mediated cell toxicity (16, 17). On the other hand, the effect of Aβ on cellular cholesterol metabolism has also been investigated (18). Our recent studies have shown that not monomeric but oligomeric Aβ affects cholesterol metabolism (19) and eventually reduces cellular cholesterol levels (20). In addition, cholesterol deficiency has been shown to promote tau phosphorylation *in vitro* (21, 22) and *in vivo* (23). These findings suggest that the involvement of cholesterol in the pathogenesis of AD is dualistic. The elevated levels of cellular cholesterol contribute to AD development by elevating Aβ secretion; however, the increasing amount of oligomerized Aβ reduces cellular cholesterol levels, which in turn may promote the progression of AD pathologies.

ApoE is one of the major apolipoproteins in the central nervous system regulating lipid metabolisms (24–27). Astrocytes and microglia are known to synthesize apoE (28, 29), which generates HDL-like particles with cellular lipids in cerebrospinal fluid (CSF) and culture media (25, 26, 30, 31). These apoE-lipid particles are assumed to supply cholesterol to neurons in an apoE receptor-mediated manner (32, 33). Previously, we have reported (34) that exogenously added recombinant human apoE promotes cholesterol release in an isoform-dependent manner. However, the mechanism underlying the isoform-dependent cholesterol release mediated by apoE remains undetermined. It is known that the majority of apoE in CSF and conditioned culture media is associated with lipids (31, 35), and that the characteristics of lipid particles generated by the addition of exogenous apolipoprotein and those generated by en-

* This work was supported by a Research Grant for Longevity Sciences 8A-1, the Program for Promotion of Fundamental Studies in Health Sciences of the Organization for Pharmaceutical Safety and Research, and Research on Brain Science from the Ministry of Health and Welfare, CREST, Japan. The costs of publication of this article were defrayed in part by the payment of page charges. This article must therefore be hereby marked "*advertisement*" in accordance with 18 U.S.C. Section 1734 solely to indicate this fact.

** To whom correspondence should be addressed: Dept. of Dementia Research, National Institute for Longevity Sciences, 36-3 Gengo, Morioka, Obu, Aichi 474-8522, Japan. Tel.: 81-562-46-2311; Fax: 81-562-46-3157; E-mail: michi@nils.go.jp.

[1] The abbreviations used are: AD, Alzheimer's disease; HDL, high density lipoprotein; apoE, apolipoprotein E; apoA-II, apolipoprotein A-II; CSF, cerebrospinal fluid; DMEM, Dulbecco's modified Eagle's medium; FBS, fetal bovine serum; PBS, phosphate-buffered saline; Tricine, *N*-[2-hydroxy-1,1-bis(hydroxymethyl)ethyl]glycine; Aβ, amyloid β-protein.

dogenous apolipoprotein are different. HDL-like particles generated by the addition of exogenous apolipoprotein AI (apoAI) (36) and apoE (34) have a low amount of cholesterol, whereas HDL-like particles formed with endogenous apoE are cholesterol-rich (37). These lines of evidence led us to determine whether the endogenous apoE-mediated cholesterol release from cultured astrocytes is isoform-specific and, if it is the case, to characterize the molecular mechanism underlying the isoform-dependent lipid release. In this study, we investigated the endogenous apoE-mediated cholesterol release from astrocytes isolated from human apoE3- and apoE4 knock-in mouse brains. We found that apoE3 has the ability to generate similarly sized HDL-like particles with less amount of apoE than apoE4. These findings may provide the basis for studies to relate cholesterol with AD pathogenesis.

EXPERIMENTAL PROCEDURES

Animals—Mice expressing human apoE4 in place of mouse apoE were generated by the gene-targeting technique taking advantage of homologous recombination in embryonic stem cells (knock-in) as described previously (38). ApoE3 knock-in mice were produced in the same manner except that the transgene carried apoE3 cDNA in place of apoE4 cDNA. The details of the generation of apoE3 mice will be described elsewhere. Postnatal day 2 mice that possess homozygous ϵ3 (3:3) or ϵ4 (4:4) allele and correctly expressing human apoE3 or apoE4 proteins, respectively, were used in this study.

Cell Culture—Highly astrocyte-rich cultures were prepared according to a method described previously (39, 40). In brief, brains of postnatal day 2 mice were removed under anesthesia. The cerebral cortices from the mouse brains were dissected, freed from meninges, and diced into small pieces; the cortical fragments were incubated in 0.25% trypsin and 20 mg/ml DNase I in phosphate-buffered saline (PBS) (8.1 mM Na_2HPO_4, 1.5 mM KH_2PO_4, 137 mM NaCl, and 2.7 mM KCl, pH 7.4) at 37 °C for 20 min. The fragments were then dissociated into single cells by pipetting. The dissociated cells were seeded in 75-cm^2 dishes at a cell density of 1×10^7 in DMEM containing 10% FBS. After 10 days of incubation *in vitro*, astrocytes in the monolayer were trypsinized (0.1%) and reseeded onto 6-well dishes. The astrocyte-rich cultures were maintained in DMEM containing 10% FBS until use.

Neuron-rich cultures were prepared from rat cerebral cortices as described previously (19). The dissociated cells were suspended in the feeding medium and plated onto poly-D-lysine-coated 6-well plates at a cell density of 2×10^5/cm^2. The feeding medium consisted of Dulbecco's modified Eagle's medium nutrient mixture (DMEM/F-12; 50:50%) and N_2 supplements. More than 99% of the cultured cells were identified as neurons by immunocytochemical analysis using monoclonal antibody against microtubule-associated protein 2, a neuron-specific marker, on day 3 of culture (41).

Quantification of Released and Intracellular Cholesterols and Phosphatidylcholines—The astrocytes in 6-well plates were washed in DMEM three times and incubated in 2 ml of DMEM for 1, 3, and 5 days at 37 °C. The conditioned culture media were removed and processed for lipid extraction. The astrocytes in the monolayer were washed in PBS three times and air-dried at room temperature. Lipids in the conditioned culture media were extracted according to methods reported previously (34, 41), with some modifications. In brief, aliquots of 1.0 ml each of the conditioned culture media were transferred to clean glass tubes containing 4.0 ml of chloroform/methanol (2:1 v/v). The organic phase was separated from the aqueous phase, washed twice by vigorous mixing with 3 ml of water, re-separated from the aqueous phase by centrifugation, and dried under N_2 gas. For extraction of intracellular lipids, dried cells were incubated in hexane/isopropyl alcohol (3:2 v/v) for 1 h at room temperature. The solvent from each plate was removed and dried under N_2 gas. The organic phases were redissolved in 400 μl of chloroform, and 150 μl of each sample was transferred onto 96-well polypropylene plates (Corning Glass) and dried under air flow. The dried lipids were then dissolved in 20 μl of isopropyl alcohol, and the contents of cholesterol and phospholipids were determined using cholesterol (Wako, Osaka, Japan) and phospholipid (Kyowa Medix, Tokyo, Japan) determiner kits, respectively.

Determination of Amount of [^{14}C]Acetate Incorporated into Cholesterol and Phosphatidylcholine—Astrocytes cultured in DMEM plus 10% FBS were washed in PBS three times and recultured in DMEM. The cultures were then treated with 37 kBq/ml [^{14}C]acetate (PerkinElmer Life Sciences) for 1, 3, and 5 days. At the indicated time points, the culture medium was quickly removed; the cells were then washed three times with cold PBS and dried at room temperature. Aliquots of 0.5 ml each of the conditioned culture media were transferred to clean glass tubes containing 2.5 ml of chloroform/methanol (2:1 v/v). For the extraction of intracellular lipids, dried cells were incubated in hexane/isopropyl alcohol (3:2 v/v) for 1 h at room temperature. The solvent from each plate was removed and dried under N_2 gas. The organic phases were redissolved in 50 μl of chloroform, and 10 μl of each sample was spotted on activated silica gel high performance thin layer chromatography plates (Merck); the lipids were separated by sequential one-dimensional chromatography using chloroform/methanol/acetic acid/water (25:15:4:2, v/v), followed by another run in hexane/diethyl ether/acetic acid (80:30:1). [^{14}C]Cholesterol and [^{14}C]phosphatidylcholine were used as standards. The chromatography plates were exposed to radiosensitive films, and each lipid was visualized and quantified with BAS2500 (Fuji Film, Tokyo, Japan). For determination of protein concentration, the astrocytes were cultured in 1 ml of distilled water containing 0.1% NaOH for 1 h, and 10 μl of each sample was processed for determination of protein concentration using a BCA kit.

Density Gradient Ultracentrifugation—After incubation in DMEM for 5 days, the astrocyte culture medium was collected, centrifuged at $1,600 \times g$ for 15 min in a 50-ml plastic tube to exclude cell debris, and adjusted to a discontinuous sucrose gradient. A discontinuous sucrose gradient was prepared in a 14 × 89-mm ultracentrifuge tube (Ultraclear, Beckman Instruments, Palo Alto, CA) from the bottom to the top, with 2 ml of sucrose at a density of 1.30 g/ml, 3 ml at 1.20 g/ml, 3 ml at 1.10 g/ml, and 4 ml at 1.006 g/ml medium. The sample in the sucrose gradient was then centrifuged in an SW41-Ti swing rotor (Beckman Instruments, Palo Alto, CA) at 4 °C for 48 h at $160,000 \times g_{av}$. Following density gradient centrifugation, 12 1.0-ml fractions were collected with a micropipette from the top gradient. The densities of the fractions were determined by measuring the weight of 100 μl of each fraction using a micropipette. The final fraction was stirred to resuspend the pellet. The lipid content in each fraction was determined as described above. The density of each fraction was determined using a density meter, DMA35N (Anton Paar, Graz, Austria).

Immunoblot Analysis—Samples of each fraction were dissolved in the sampling buffer consisting of 100 mM Tris-HCl (pH 7.4), 10% glycerol, 4% SDS, 10% mercaptoethanol, and 0.01% bromphenol blue and analyzed by 12.5% Tris/Tricine SDS-PAGE as reported previously (42). The separated proteins were transferred onto Immobilon membranes with a semidry electrophoretic transfer apparatus (Nihon Eido, Tokyo, Japan) using a transfer buffer (0.1 M Tris, 0.192 M glycine, and 20% methanol). Blots were probed for 4 h at room temperature with a goat anti-apoE polyclonal antibody, AB947 (1:2,000; Chemicon, Temecula, CA) and a goat anti-apoJ antibody (1: 2,000; Rockland, Gilbertsville, PA). Band detection was carried out with an ECL kit (Amersham Biosciences). For determination of the concentration of apoE released into the culture medium, signals corresponding to apoE of each sample in the immunoblot membrane were quantified by densitometry with NIH image software, with varying concentrations of synthetic apoE protein (Wako, Tokyo, Japan) as standards. Standard signals were demonstrated to be linear in the range of apoE protein amounts from 0 to 2 μg per lane. The apoE concentrations in the conditioned culture media within this range were used for analysis. For detection of the oligomeric apoE protein in the conditioned culture media, Western blot analysis was performed under nonreducing conditions. Aliquots of each conditioned culture medium of apoE3- and apoE4-expressing astrocytes were mixed with the same volume of the 2× nonreducing Laemmli buffer consisting of 100 mM Tris-HCl (pH 7.4), 10% glycerol, 4% SDS, and 0.01% bromphenol blue, but no β-mercaptoethanol, and analyzed by Western blotting as described above.

Size Determination of Lipoprotein Particles—The conditioned culture media of astrocytes expressing human apoE3 and apoE4 were concentrated 5-fold using a Centriprep-YM10 tube (Millipore, Bedford, MA) by centrifugation in a JA-12 rotor using a Beckman J-25I ultracentrifuge at 4 °C for 40 min at $3,000 \times g$. After centrifugation, the sample was subjected to density gradient ultracentrifugation with a discontinuous sucrose gradient as described above. Two milliliters of the HDL fraction (fraction number 4) in a Centricon YM10 tube (Millipore) was further concentrated to 200 μl in a JA-20.1 rotor using a Beckman J-25I ultracentrifuge at 4 °C for 2 h at $5,000 \times g$. The concentrated conditioned culture medium was then subjected to nondenaturing 4–20% TBE (pH 8.3)-buffered PAGE to evaluate the particle size heterogeneity of the apoE fractions. Ten microliters of apoE-lipid particles (unboiled and nonreduced) containing 10% sucrose and 0.02% bromphenol blue was applied onto 4–20% gradient gel. Native high molecular weight protein standards (Amersham Biosciences) were used as size standards

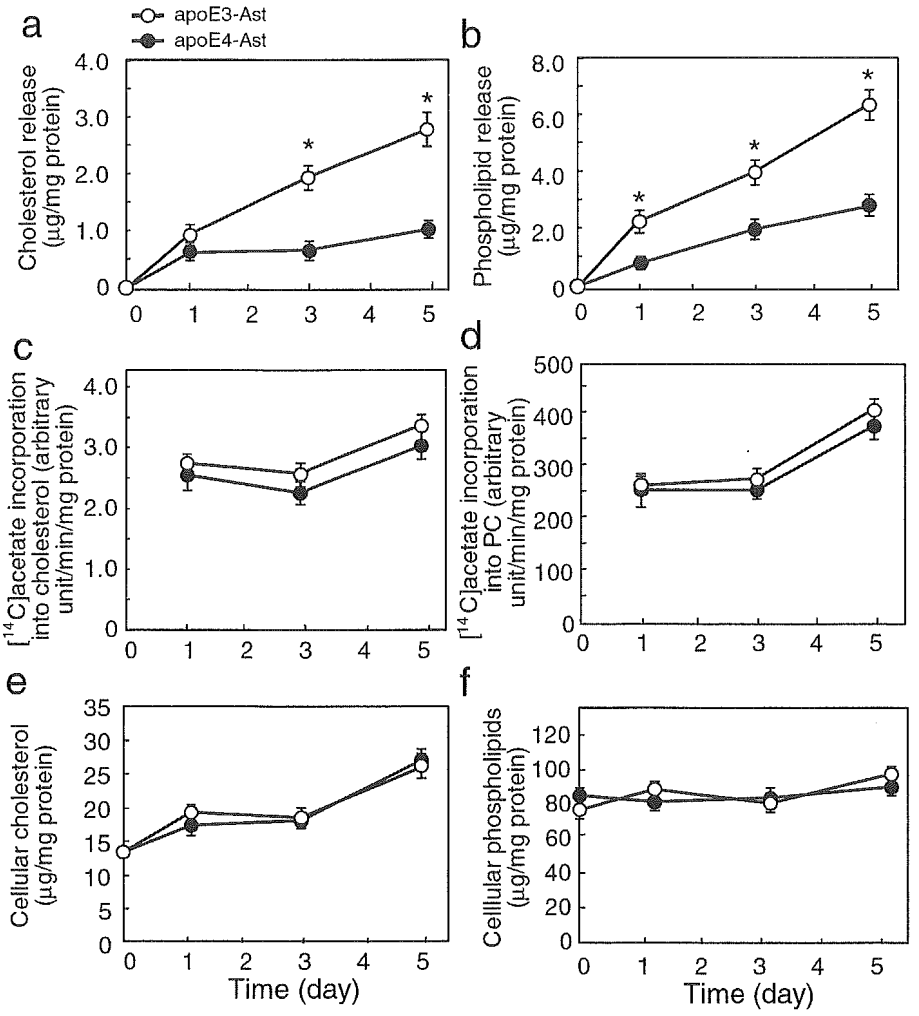

FIG. 1. **Characterization of lipid metabolism in cultured astrocytes prepared from human apoE3 and apoE4 knock-in mouse brains.** Astrocyte-rich cultures were prepared as described under "Experimental Procedures." Three-week-cultured astrocytes were washed three times with DMEM and incubated in DMEM. At the time points indicated, the lipids released into the medium and the intracellular lipids were extracted and analyzed as described under "Experimental Procedures" (*a*, *b*, *e*, and *f*). For determination of the synthesis rates of cholesterol and phospholipids, the cultured astrocytes were washed three times with DMEM, followed by incubation with [^{14}C]acetate for 2 h at 37 °C. The cells were then washed in cold PBS three times, and the amount of [^{14}C]acetate incorporated into cholesterol and phosphatidylcholine was determined as described under "Experimental Procedures" (*c* and *d*). The amounts of cholesterol (*a*) and phospholipids (*b*) from apoE3-expressing astrocytes (○) were significantly greater than those from apoE4-expressing astrocytes (●), respectively, and there were no significant differences in cellular cholesterol/phospholipids concentrations (*e* and *f*) or the rate of cholesterol/phosphatidylcholine synthesis (*c* and *d*) between apoE3- and apoE4-expressing astrocytes. Data are means ± S.E. for 4 samples. *, $p < 0.001$ *versus* apoE4-expressing astrocytes. Six independent experiments show similar results.

(43). Electrophoresis was performed at 4 °C with a prerun of 15 min at 125 V before the entry of samples into the stacking gel, followed by migration at 100 V for 8 h. The separated apoE that migrated as a lipid-apoE complex was transferred onto Immobilon membrane with a semidry electrophoretic transfer apparatus (Nihon Eido, Tokyo, Japan) using a transfer buffer (0.1 M Tris, 0.192 M glycine and 20% methanol). Separated proteins were probed for 4 h at room temperature with a goat anti-apoE polyclonal antibody, AB947 (Chemicon, Temecula, CA) (1:2000). ApoE protein was detected using an ECL kit (Amersham Biosciences). The mean apoE-lipid particle size was obtained based on the migration of the size standards, which were stained by 0.5% Ponceau S (Sigma) and 1% acetic acid in distilled water.

Statistical Analysis—StatView computer software (Macintosh) was used for statistical analysis. Statistical significance of differences between samples was evaluated by the Student's *t* test.

RESULTS

The apoE3- and apoE4-expressing astrocytes became confluent 7 days after replating and appeared morphologically comparable. The time-dependent curves for the release of cholesterol and phospholipids from cultured astrocytes expressing human apoE3 and apoE4 are shown in Fig. 1, *a* and *b*, respectively. We found that the amounts of cholesterol (Fig. 1*a*) and phospholipids (Fig. 1*b*) released from cells of both genotypes increased in a time-dependent manner and that the amounts of these lipids released from apoE3-expressing astrocytes were significantly higher than those from apoE4-expressing astrocytes at days 3 and 5, when compared on the basis of cellular protein. In contrast, the levels of [^{14}C]acetate incorporation into cholesterol and phosphatidylcholine in both apoE3- and apoE4-expressing astrocytes were at similar at each time point (Fig. 1, *c* and *d*). Similarly, the total amounts of cellular cholesterol and phospholipids in both genotypes of astrocytes were similar at each time point (Fig. 1, *e* and *f*).

We next determined the amounts of apoE3 and apoE4 released into each culture medium. Western blot analysis of the conditioned culture media of apoE3- and apoE4-expressing astrocytes at culture days 1, 3, and 5 shows that the total amount of apoE released into the culture media of both apoE3- and apoE4-expressing astrocytes increased with culture time (Fig. 2, *a* and *b*). The densitometric analysis of these signals shows that comparative amounts of apoE were released from apoE3- and apoE4-expressing astrocytes (Fig. 2*b*).

The characteristics of the lipid particles released into the serum-free media from cultured astrocytes were examined. The results of density gradient ultracentrifugation of the cultured media of apoE3- and apoE4-expressing astrocytes, shown in Fig. 3, indicate that the lipid distribution in each sample contains two peaks. They show that most of the cholesterol and phospholipids are distributed similarly in the fractions with densities of 1.04–1.13 (fractions 3–5). They also show that smaller amounts of cholesterol and phospholipids are distributed in the fractions having densities of 1.14–1.21 g/ml (fractions 8 and 9). These results show that the major parts of cholesterol and phospholipids were present in the lighter density fractions 3–5, and the minor parts of these lipids were present in the heavier density fractions 8 and 9, the densities of which corresponded to those of HDL. Next, we performed immunoblot analysis of each fraction using anti-apoE and anti-apoJ antibodies. ApoE3 and apoE4 were detected mainly in fractions 4 and 5 of each sample of the conditioned culture

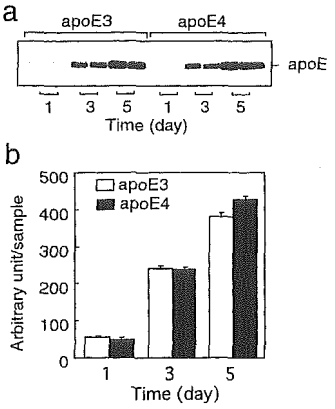

FIG. 2. **Amount of apoE protein released into the conditioned culture media of apoE3- and apoE4-expressing astrocytes.** Astrocyte-rich cultures were prepared as described under "Experimental Procedures." Before experiments, the cells were washed three times with DMEM and cultured in DMEM. At the time points indicated, the lipids released into the medium were extracted and analyzed as described under "Experimental Procedures." The aliquots (5 μl) from each sample were subjected to immunoblot analysis using the polyclonal anti-apoE antibody, AB947, as the primary antibody (*a*). The intensity of each band was quantified by densitometric analysis using NIH imaging software for Macintosh (*b*). The amount of apoE released into the culture media from apoE3-expressing astrocytes was similar to that from apoE4-expressing astrocytes. Four independent experiments show similar results.

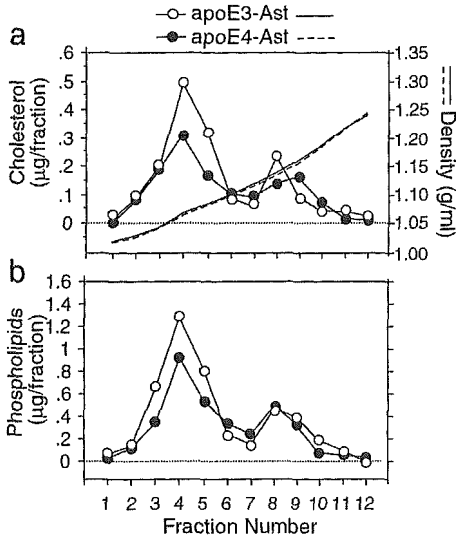

FIG. 3. **Density gradient analysis of lipid particles released from astrocytes.** Three-week-cultured astrocytes plated in 6-well dishes were maintained in DMEM containing 10% FBS (324 μg/ml cholesterol). The astrocytes were rinsed three times with fresh DMEM and incubated in DMEM for 5 days. The culture medium was collected and centrifuged at 1,600 × *g* for 15 min to exclude cell debris. The supernatant was collected and subjected to the initial discontinuous density gradient prepared with sucrose solutions as described under "Experimental Procedures." After centrifugation, fractions were collected and analyzed for their cholesterol (*a*) and phospholipid (*b*) contents. The density of each fraction was also determined using a density meter, DMA35N (*a*). *apoE3-Ast*, apoE3-expressing astrocytes; *apoE4-Ast*, apoE4-expressing astrocytes. Six independent experiments showed similar results.

media of apoE3- and apoE4-expressing astrocytes, which is consistent with the major peak of lipid distribution, as shown in Fig. 4, *a* and *b*, respectively. In contrast, apoJ in each sample of the conditioned culture media of apoE3- and apoE4-expressing astrocytes was detected in fractions 6–11, which are distinct from those containing apoE (Fig. 4, *a* and *b*). The distributions of apoE and apoJ across the fractions of each sample as quantified by densitometric analysis are shown in Fig. 4*c*,

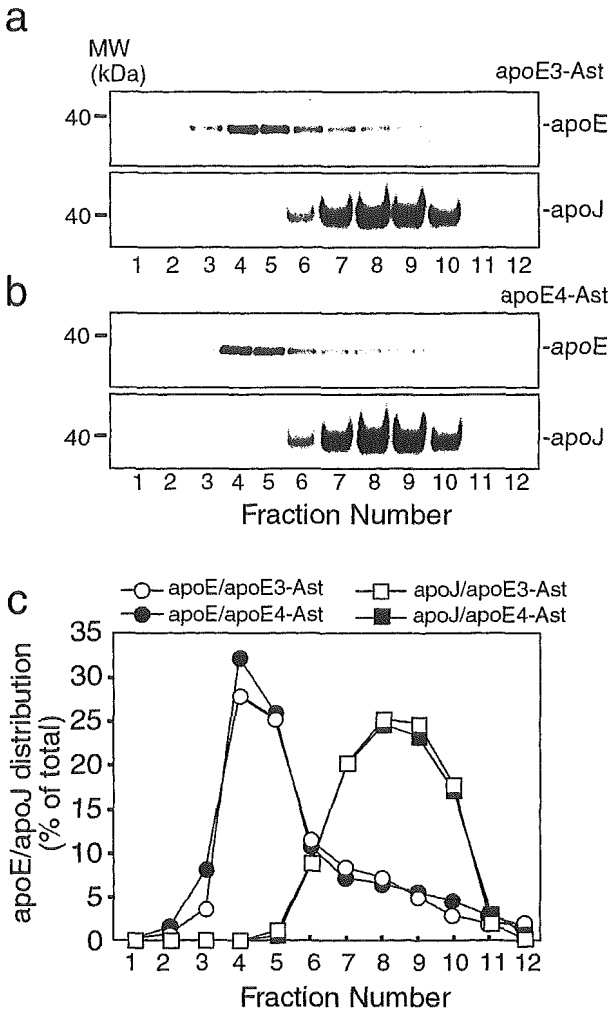

FIG. 4. **Distribution of apoE3 and apoE4 across the fractions separated by density gradient ultracentrifugation.** Twelve fractions obtained from the culture media of apoE3- and apoE4-expressing astrocytes as described in Fig. 3 were used for determination of the distribution of apoE and apoJ. Aliquots of 10 μl from each fraction were mixed with the same volume of sample buffer and subjected to SDS-PAGE. The separated proteins from the culture media of apoE3- (*a*) and apoE4-expressing astrocytes (*b*) were immunoblotted with an anti-apoE antibody and an anti-apoJ antibody. To determine the distribution pattern of apoE (○ and ●) and apoJ (□ and ■) across the fractions, immunoblot membranes were subjected to scanning, and the intensity of each band was determined by densitometric analysis using computer software (*c*). *apoE3-Ast*, apoE3-expressing astrocytes; *apoE4-Ast*, apoE4-expressing astrocytes. Six independent experiments show similar results.

indicating the difference in distribution between apoE and apoJ.

In addition, because we found that neurons synthesize and secrete apoJ to form HDL-like particles without secretion of apoE, we characterized the apoJ-mediated lipid release from neurons to compare it with that from astrocytes. The apoJ-mediated lipid release into the conditioned media of cultured neurons was found to be distributed across the fractions at densities from 1.092 to 1.180 g/ml, which is similar to that of apoJ-mediated lipid release from astrocyte cultures (Fig. 5). The distribution peaks of apoJ (Fig. 5*a*), cholesterol (Fig. 5*b*), and phospholipids (Fig. 5*c*) across the fraction densities were found to be identical at 1.127 g/ml. These results show that apoJ-containing lipoproteins in both conditioned media of cultured neurons and astrocytes are heavier than those generated by apoE in the conditioned media of cultured astrocytes and that the characteristics of apoJ-containing lipoproteins gener-